Reviewer 1

Summary:
The authors collected samples of functionalized organic compounds from a wildfire using an aircraft platform. Particles were collected on filters and sampled using LC and GC techniques offline, while gas phase compounds were collected in adsorbent tubes and sampled primarily using the LC method offline. The authors illustrate the importance of sulfide compounds, concluding that sulfides are formed through secondary chemistry and are a major contributor to CHONS compounds after plume aging. They discuss possible sources of these sulfur compounds. The measurements and analysis are quite interesting, and definitely of interest to others researching organic compounds (particularly lower volatility gases and particulate speciation). I have one major issue with how the authors quote numbers for relative contributions of sulfide and CHONS in the abstract, rather than using (dilution corrected) absolute concentrations to really prove that secondary formation is occurring. The data supporting abstract-level conclusions needs to be presented in the main paper, rather than the SI figures. This issue can be resolved through reorganization, and after addressing that along with my other comments, I would recommend for publication.

> We thank the reviewer for their supportive comments. We modified our figure presentation and our discussion of the data in the abstract and manuscript to address both the absolute and relative contributions from CHONS and sulfide species. We discuss our edits in detail in the line-by-line responses below.

Specific Comments:
Abstract, Sect 3.1, 3.2, etc.: In several places in the main text and figs including the abstract, Sects. 3.1 and 3.2, you present data by relative abundance of each screen. You present that the relative contribution of sulfides increases with plume age, and quote those numbers in the abstract in the context of saying sulfides are formed through secondary chemistry from S/IVOCs. However, the change in relative contribution alone could have several causes: sulfides could be being formed from chemistry in the plume (which is what you show with Fig. S6A with the CO-normalized plots), or sulfides could just be evaporating less than other functional groups and thus becoming relatively more important. Like I said, with Fig. S6A you show that the absolute concentration (when dilution corrected) is increasing, so there is some chemical formation, but you're not presenting your data or quoting the right numbers in the abstract to back up this conclusion. I believe this conclusion is really the main conclusion that you're trying to show with this work, and that's why you go on to a lot of discussion of possible secondary sources of sulfides in Sect. 3.5. But you're only showing it with an SI figure. This is a major issue with the organization of manuscript, in my opinion. And in the abstract, the quoted numbers seem potentially misleading to me. You present the numbers for relative increase (which on their own don't necessarily mean secondary formation, and might not quantitatively represent the amount of secondary formation), but the context is that sulfides are being formed through secondary chemistry. I think you need to be showing CO-normalized data in the main paper figs and quote those numbers in the abstract. As an imprecise use of data to back up conclusions in the abstract, I say it's a major issue, but it should be easy to resolve and it won't change your conclusions.

We thank the reviewer for bringing up this important distinction. In Figure 1 and the associated discussion, we showed the contribution of CHONS and sulfide species in terms of their relative prevalence, to contrast changes in CHONS and sulfide contributions with other compound classes and functional groups in the observed complex mixture of emissions and transformation products. We agree that changes in relative contributions could be driven by a number of factors, such as chemical formation and different relative rates of evaporation that could vary between compound classes and functional groups. For this study, we were interested in looking at both the absolute formation of CHONS and sulfide species *and* the evolution of the overall complex mixture of compound classes/functional groups. As a result, we chose to include relative contributions of compound classes and functional groups in the main text, and in the interest of space, absolute contributions corrected for dilution (using carbon monoxide measurements) in the SI. We recognize that both ways of presenting results (i.e. as relative or absolute contributions) are valuable for different purposes. In both cases, the observed trends in CHONS and sulfide contributions were similar. Both approaches showed an overall growing contribution of CHONS and sulfides from screen 1 to 4, peaking at screen 4.

To address the reviewer's concern and provide more information the reader in the main text, we added an inset to Figure 1 that shows the absolute contributions of CHONS and sulfides with plume age (using dilution-corrected abundances). We added an inset rather than replacing the full figure because we did not want to lose the information presented in the current Figure 1A-C on the evolution of the complex mixture as a whole. In Figure 1's caption, we added an additional reference to the SI figures that show all compound classes and functional groups by absolute dilution-corrected abundance. We also note that we already show dilution corrected values for the gas-phase data in Figure 4. Also, in the abstract (lines 21-22 and 24-26) and in other instances where we reported the change in relative contribution of CHONS and sulfide species, we added a mention of their increase in dilution-corrected abundance. Finally, we included a note to the results section that draws attention to both methods of tabulation (lines 187-192).

Line 180: Again, the increase in relative abundance of sulfides among CHONS species doesn't tell us whether sulfides are being formed, or if they're just evaporating/reacting more slowly than other functional groups. But the discussion here all assumes secondary formation. This is the same as my first comment, really.

This concern is addressed above. At line 186-187, we added a sentence to show increases in absolute abundance (corrected for dilution using CO) to more strongly support the conclusion of CHONS formation. Similar additions were made when sulfides were discussed (lines 207-208).

Fig. S5 and elsewhere: What is the difference between abundance and occurrence? I don't see it explained anywhere, so I don't know what point you're trying to make by showing plots of occurrence.

The results shown in select SI figures tabulated by both abundance and occurrence are for comparison purposes only. The results tabulated by abundance are the ones discussed throughout the manuscript. However, due to uncertainty in ionization efficiency of individual multifunctional compounds within the complex mixture, we provide the reader with supporting data on the detailed distribution of compound classes, volatility ranges, and functional groups by occurrence as well (i.e. by number of compounds in each category). Trends in most cases were similar, suggesting that the interpretation of the abundance-weighted results was not substantially skewed by differences in ionization efficiency. This was originally discussed briefly at the end of SI Section S4. To address the reviewer's comment, we added a mention of the specific figures in the SI for which we showed both abundance-weighted and occurrence-based results for emphasis (SI lines 287-289). We also added a reference to Section S4 in the captions of the relevant figures, to draw attention to the discussion (Figures S5, S6, S8, S9).

Line 195: How are you estimating the volatility of the compounds? It looks like you might be explaining in line 201 (and Fig. S8, S9 captions), but it would be good to give that detail in the methods section before you start discussing volatilities here.

Thank you for the suggestion. We added a few sentences to the Materials and Methods section to discuss this for adsorbent tubes and filters (clarified lines 113-124, added lines 127-130 and lines 157-162).

Line 82: Could you provide a little more info about the two-plume structure of the fire? Was it two spots of active burning/smoldering, and if so how close were they, or was it one spot that evolved two plumes with different ages? Mainly, I just want to know if both plumes in a given screen were sampled at approximately the same age. Maybe you could indicate an approximate location of the start of the second plume in Fig S1.

Based on analyses of satellite imagery and ground meteorological measurements, the NP was likely from the same source as the South Plume (SP). The NP likely occurred due to a switch in wind direction just prior to sampling. This means that the NP may be slightly older than the SP—we estimate this age difference to be <30 minutes, so they are roughly the same age. We added a brief mention of the ages of the plumes to the caption of Figure S1. Because the source of the NP was not identified via satellite imagery, it is not included explicitly in Figure S1 (this is mentioned in the caption).

Line 87: What were the altitudes sampled in each screen?

The average altitude of samples varied ~650-1650 m for adsorbent tubes (collected on distinct low and high altitude passes through the plume), and ~900-1600 m for filters (one filter per screen). Average altitudes were originally shown in Table S1, and we

added a reference to this table at line 90 to ensure that this information is readily found by readers.

Line 214: There are a lot of acronyms and methods involved in your analysis (not a criticism, just an observation!), so it can be a little tricky to follow that you're switching now from discussing the particle phase that was sampled via filters to discussing the gas phase sampled via adsorbent tubes. I'd recommend just adding a quick note here to say this more explicitly, that in order to try to understand the particle phase filter measurements presented earlier, you're now doing targeted analysis of the gas phase sampled via adsorbent tubes.

We edited this sentence to make the transition clearer to readers (line 246-248).

Line 300: Could you discuss whether or not there are any sulfur-containing compounds included in any fire suppressant materials that could have been deposited on this fire?

Smoke from this fire was sampled when the fire was less than 1 hour old and there had been no prior active fire suppression activities. Fire suppressant from past applications could have deposited on forest surfaces and re-volatilized, though historically, fire suppressants are not heavily used this region due to the abundance of lakes in the area. Also, this region uses water almost exclusively as a fire retardant. While it is possible that non-water fire suppressants were applied historically, the exact type and quantity are uncertain. It appears that one of the most commonly used fire suppressants in Canada today contains ammonium phosphate salts, sometimes with sulfate-containing salts mixed in. The exact composition of a few example fire suppressants that we searched for were proprietary, so the contribution of sulfate salts is unknown, but likely minor compared to that of phosphate salts. The contribution of any sulfur-containing compounds from fire suppressants to the observed gas/particle-phase species is therefore expected to be minor or negligible (if 100% water was used). We added a sentence to briefly mention fire suppressants at lines 366-368.

Sects. 3.4 and 3.5: Both of these sections are entirely 'discussion' of what could be explaining your data, and not presentation of your 'results'. Thus, they don't need to have their own sections under your 'results and discussion' header. You should either move them up into the previous sections where you actually present the results you're discussing, or change Sect. 3 to just 'Results' and have Sect. 4 be "Discussion" including these two sections (and make Conclusions be Sect. 5).

Thank you for the suggestion. We turned section 3 into "Results", moved 3.4-3.5 to "Discussion" (now 4.1-4.2), and adjusted the "Conclusions" to become section 5.

SI line 75: extra s in VOCs

This has been corrected.

Fig. S9: Should include a legend for screens 1-5, as in Fig S5, for completeness

We added a legend to panel A.

Section S5: This whole section is great! Provides really nice context for interpreting all of the measurements you present throughout the manuscript. I'd advocate for moving Sect. S5 to the end of the main paper methods section.

We thank the reviewer for the supportive comment. We felt that the comprehensive discussion of the differences between LC-ESI and GC-APCI methods was better suited to the SI, so that we could include several numerical details that described the types of compounds accessible with each technique without bogging down the reader with too many supplemental details in the main text. However, we have taken the reviewer's recommendation and added a short paragraph to the end of the Materials and Methods section that introduces the longer discussion in the SI (lines 148-156).

Fig 1A along with Section S5: So Fig. 1A is really showing the relative abundance of the part of OA that could be sampled using the LC-ESI-MS method. You say LC is better for larger, more polar, more functionalized, less volatile compounds. How could this be biasing your percentages in Fig. 1A? E.g., maybe the sulfur compounds tend to be lower volatility and better sampled, while some less oxidized, less polar CHO compounds are poorly sampled? Some discussion would be useful, especially if you bring Sect. S5 to the main paper.

The LC-ESI methods used in this work are better suited for detecting more functionalized and polar compounds present in the OA sampled on PTFE filters (IVOCs-SVOCs included). LC-ESI (using both positive and negative mode) is known to be effective for a wide range of species that contain at least one oxygen atom or one nitrogen atom (in addition to combinations of sulfur with oxygen and/or nitrogen, and combinations of all three heteroatoms), making it conducive for measurements of biomass burning emissions and transformation products. While these methods exclude CH and CHS species (i.e. fully reduced hydrocarbons and compounds containing reduced sulfur only), this was acknowledged in the text and filter samples were run on the GC-APCI to explore the contribution of CH and CHS species to the particle-phase. From the GC-APCI analysis of particle-phase samples, we observed a greater contribution from CHO species and relatively lower fractions of the other heteroatom-containing groups, including CHS. This is likely because these other heteroatom-containing species were less GC-amenable, and thus were lost during solvent extraction, lost to the GC inlet, or lost to the GC column during analysis.

Both LC-ESI and GC-APCI methods have column transmission and ionization strengths and weaknesses for different classes of compounds. The focus of this manuscript was on the formation of functionalized products from biomass burning emissions, so the LC-ESI approach and results were more extensively used because they were better suited for highly-functionalized species. The compositional percentages shown in Figure 1A are shifted in an absolute sense by the exclusion of CH and CHS compounds, but particle-phase CH and CHS species were outside the scope of this study. We did not up including

the full Section S5 in the main text, but to address the reviewer's concerns we added a shorter paragraph summarizing Section S5 (lines 148-156) and included an acknowledgement in that section that LC-ESI methods excluded CH and CHS species.

Title: It would be good to change the last word from "compounds" to "organic compounds" to make it more clear that organic compounds are the focus.

Agreed, we have edited our title accordingly.

Reviewer 2

ACP manuscript 2020-619 reports on the detailed chemical composition of gas- and particle-phase samples collected from a boreal forest fire under ambient conditions. Samples were analyzed using gas and liquid chromatography (GC, LC) with detection by high-resolution and tandem mass spectrometry (MS, MS/MS). The focus of the analysis was on organic compounds, particularly those containing carbon, hydrogen, oxygen, nitrogen, and/or sulfate functionalities ("CHONS"); including as a function of plume age. Targeted and non-targeted approaches were used. Using both GC and LC allowed analysis of less polar (GC) and more polar/more functionalized compounds (LC) than could be achieved using a single method. Results are largely discussed in the context of elemental composition, with less focus on compound identification. It was observed that during aging particle-phase CHO compounds became less abundant, while particle-phase CHON(S) became significantly more abundant. The paper also presents precursors and pathways leading to the formation of observed sulfides included among the CHONS compounds. The paper is well written and presents interesting analysis and results that have not been presented before. The results, implications, and approach should be of interest to ACP readers. The methods are generally well described and could be reproduced based on the information provided in the SI. A few comments are provided below, both technical and editorial in content. The most significant comment on the technical side is that there are places in the manuscript where it is not clear if the compound volatility classes are being appropriately defined (i.e., based on published saturation vapor concentration ranges) based on the observed gas- and particle- phase distributions.

We thank the reviewer for their supportive comments. We have addressed each of their comments below, including a discussion of volatility.

Technical Comments:

line 96: Is the uncertainty on the MCE values really +/- 0.4? That seems very large, given the typical range of ambient MCE values.

We thank the reviewer for pointing this out. This was originally a typo. This has been revised in the main text to say +/- 0.01.

Starting on line 104, the description of the volatility range of compounds sampled is a little unclear. It seems that compounds that are largely in the gas phase at OA mass loadings of 10-30 ug/m3 would be classified as I/VOCs and not SVOCs. On the other end of the spectrum, C10-20

compounds that are largely in the gas phase may be in the VOC range (and not necessarily in the I/SVOC range).

We thank the reviewer for pointing out this possible point of confusion for readers. We would like to clarify that all volatility bins (VOC, IVOC, SVOC, LVOC, ELVOC) were based on fixed values of saturation mass concentration, C* (as discussed in e.g. Donahue et al., 2009, and Murphy et al., 2014) at typical OA mass loadings (e.g. 18-22 ug/m^3 of OA during the adsorbent tube sampling times). In these conditions, VOCs extend up through hydrocarbons (i.e. CH compounds) with 11 carbon atoms (specifically compounds with an n-alkane-equivalent volatility of C_{11}). IVOCs include hydrocarbons with 12-18 carbon atoms, which are shown to equilibrate primarily to the gas-phase in outdoor conditions at the observed particle loadings. SVOCs, which begin with hydrocarbons with 19 carbon atoms, are present in both the gas- and particle-phase, with hydrocarbons less than C_{22}-C_{23} existing predominantly in the gas-phase in the observed conditions. To estimate gas-particle partitioning of these C_{22}-C_{23} compounds, we used the partitioning coefficient calculation described in Donahue et al., 2009 (Equation 1 in the SI), which relates the effective saturation mass concentration of mixture components to the overall OA mass loading. This is discussed in the SI (lines 230-243) and in Table S2.

To ensure that our volatility calculations and definitions were clear, we edited the Materials and Methods discussion of volatility for adsorbent tube samples (lines 113-130), and added more discussion of the volatility calculations for filter samples (lines 157-162). We also added a note at line 123 to direct readers to Section S3 and Table S2 in the SI, which discuss volatility further.

References:

- Donahue et al., "Atmospheric organic particulate matter: From smoke to secondary organic aerosol." *Atmospheric Environment,* 2009
- Murphy et al., "A naming convention for atmospheric organic aerosol." *Atmospheric Chemistry and Physics,* 2014

This continues in 204-205, with discussion of "particle-phase" IVOCs; it isn't clear why at mass loadings of 10-30 ug/m3 of OA, particle-phase IVCOs would be above detection limits. By definition, such compounds are largely in the gas phase except at high OA loadings.

The IVOCs discussed here refer specifically to functionalized particle-phase compounds, where polarity can affect partitioning behavior. We have observed particle-phase IVOCs in several past studies by our group (e.g. Ditto et al., 2018, Ditto et al., 2020) and others (e.g. studies of isoprene oxidation products that show species like 2-methyltetrols and methylglyceric acid in the particle phase, e.g. Carlton et al., *Atmos. Chem. Phys.,* 2009), which could be attributed to the presence of more polar and water-soluble compounds that are commonly observed in organic aerosol.

References:

- Ditto et al., "An omnipresent diversity and variability in the chemical composition of atmospheric functionalized organic aerosol." *Communications Chemistry*, 2018
- Ditto et al., "Nontargeted Tandem Mass Spectrometry Analysis Reveals Diversity and Variability in Aerosol Functional Groups across Multiple Sites, Seasons, and Times of Day." *Environmental Science and Technology Letters*, 2020
- Carlton et al., "A review of Secondary Organic Aerosol (SOA) formation from isoprene." *Atmospheric Chemistry and Physics,* 2009

In lines 241-243, it is suggested that compound types that have widely been observed in gas-phase smoke samples, evaporated with dilution. While a fraction of the directly emitted gas-phase compounds may partition to the particles, many of the compounds in the classes listed are not expected to contribute directly to the particle phase. Such compounds first undergo chemical transformation to create lower volatility products and then condense to the particle phase. It is not clear whether the parent compounds and their products would be observed as the same mass fragments using the techniques described.

We thank the reviewer for pointing out this potentially confusing phrasing. In our original text, we intended to discuss the possibility of evaporation of these compound classes from particle-phase emissions, in addition to direct gas-phase emissions of these compound classes. Evaporation of particle-phase species to the gas-phase has been observed in many past studies of IVOCs and SVOCs (e.g. those referenced at line 267, in addition to other studies on the semivolatile nature of primary organic aerosol such as Robinson et al., *Science,* 2007). We have edited this section in the text to ensure that our intended meaning is clear (line 276-278).

References:

- Robinson et al., "Rethinking Organic Aerosols: Semivolatile Emissions and Photochemical Aging." *Science*, 2007

The discussion of volatility and partitioning needs to be carefully reviewed throughout the manuscript, and revised for accuracy, consistency, and clarity.

We have carefully gone through the text to ensure that our discussion of volatility and partitioning was clear, and have edited language to improve clarity where needed.

line 134: What were the "strict" QC/QA guidelines for peak retention? These are not defined in the manuscript or SI.

A brief discussion of QA/QC was originally included in the SI in section S3.1. We added a note in the main text so readers know to consult this section for QA/QC information (line 145). We also added "QA/QC" to the section titles for S3.1 and S3.2 to emphasize this discussion. The QA/QC methods are discussed more thoroughly in the following publications referenced in the manuscript:

- Ditto et al., "An omnipresent diversity and variability in the chemical composition of atmospheric functionalized organic aerosol." *Communications Chemistry*, 2018
- Ditto et al., "Nontargeted Tandem Mass Spectrometry Analysis Reveals Diversity and Variability in Aerosol Functional Groups across Multiple Sites, Seasons, and Times of Day." *Environmental Science and Technology Letters*, 2020

line 198: Is quantification of filter species affected at all by compound volatility? Or is the extraction process sufficient to extract the presumed ELVOCs with reasonable recovery?

We expect that the filter extraction process across the reported volatility ranges should be fairly uniform. It is possible that the solvent extraction is slightly more or less effective for different chemical functionalities (i.e. compound classes), though upon testing, we did not observe any distinct trends with compound class, and the selected solvent (methanol) has been used extensively in past work (e.g. Riva et al., 2016, Surratt et al., 2008, Ng et al., 2008) that studied similarly functionalized organic aerosol species. We added a mention of this to the Supporting Information (SI line 250-252).

References:

- Riva et al., "Characterization of organosulfates in secondary organic aerosol derived from the photooxidation of long-chain alkanes." *Atmospheric Chemistry and Physics,* 2016
- Surratt et al., "Organosulfate Formation in Biogenic Secondary Organic Aerosol." *Journal of Physical Chemistry A,* 2008
- Ng et al., "Secondary organic aerosol (SOA) formation from reaction of isoprene with nitrate radicals (NO3)." *Atmospheric Chemistry and Physics,* 2008

SI line 48: How was the collection efficiency of the AMS determined? Lim et al. 2019 ACP demonstrated the significant impact of CE on

The collection efficiency of the AMS was determined using the method of Middlebrook et al. (Aerosol Science and Technology, 2012). The collection efficiency was also estimated by comparing the total mass concentrations with those derived from the UHSAS (Ultra-high sensitivity aerosol spectrometer). UHSAS volume concentrations were converted to mass concentrations using densities weighted by the AMS components. Both methods yielded similar results. In addition, there was no evidence to suggest that the AMS collection efficiency changed in and out of the fire plumes, which is consistent with previous AMS wildfire deployments (e.g. in the published data sets associated with ARCTAS – Hecobian et al., 2011; Cubison et al., 2011; SEAC4Rs – Liu et al., 2016; SCREAM – May et al., 2015). We have added a mention of these methods to the Supporting Information (SI line 47-52).

References:

- Middlebrook et al., "Evaluation of Composition-Dependent Collection Efficiencies for the Aerodyne Aerosol Mass Spectrometer using Field Data." *Aerosol Science and Technology*, 2012
- Hecobian et al., "Comparison of chemical characteristics of 495 biomass burning plumes intercepted by the NASA DC-8 aircraft during the ARCTAS/CARB-2008 field campaign." *Atmospheric Chemistry and Physics*, 2011
- Cubision et al., "Effects of aging on organic aerosol from open biomass burning smoke in aircraft and laboratory studies." *Atmospheric Chemistry and Physics*, 2011
- Liu et al., "Agricultural fires in the southeastern U.S. during SEAC^{4}RS: Emissions of trace gases and particles and evolution of ozone, reactive nitrogen, and organic aerosol." *Journal of Geophysical Research: Atmopheres*, 2016
- May et al., "Observations and analysis of organic aerosol evolution in some prescribed fire smoke plumes." *Atmospheric Chemistry and Physics*, 2015

SI line 83: I'm assuming that the field blanks were used to correct for background, and not to reduce background as stated here.

Yes, blanks were used to account and correct for any contamination in the sampling and analytical systems. We have changed the word "reduce" to "correct for", now at SI line 87.

Editorial Comments: line 62: In this context, what is meant by "unprecedented"? Is it in reference to the analytical techniques used? Or the extent of chemical composition data obtained? Other?

In this context, we used "unprecedented" to mean that the analytical methods and degree of chemical speciation were novel. We removed the term to reduce possible confusion.

line 113: No hyphen is needed between "gas" and "phase" (also in line 224 in the SI).

These have been corrected.

SI line 75: remove one of the "s" on "VOCss"

Corrected.

line 129: "mode" should be plural

Corrected.

SI line 295: suggest to move the Kroll et al reference as it suggests the values themselves (rather than the approach) are from Kroll et al.

We moved the reference so that it appears earlier in the sentence.

Atmospheric Evolution of Emissions from a Boreal Forest Fire: The Formation of Highly-Functionalized Oxygen-, Nitrogen-, and Sulfur-Containing Organic Compounds

Jenna C. Ditto[1], Megan He[1], Tori N. Hass-Mitchell[1], Samar G. Moussa[2], Katherine Hayden[2], Shao-Meng Li[2], John Liggio[2], Amy Leithead[2], Patrick Lee[2], Michael J. Wheeler[2], Jeremy J.B. Wentzell[2], Drew R. Gentner[1,3,*]

[1] Department of Chemical and Environmental Engineering, Yale University, New Haven, CT, 06511, USA; [2] Air Quality Research Division, Environment and Climate Change Canada, Toronto, Ontario M3H 5T4, Canada; [3] Solutions for Energy, Air, Climate and Health (SEARCH), School of the Environment, Yale University, New Haven CT 0651, USA

* Correspondence to: drew.gentner@yale.edu

Abstract

Forest fires are major contributors of reactive gas- and particle-phase organic compounds to the atmosphere. We used offline high resolution tandem mass spectrometry to perform a molecular-level speciation of gas- and particle-phase compounds sampled via aircraft from an evolving boreal forest fire smoke plume in Saskatchewan, Canada. We observed diverse multifunctional compounds containing oxygen, nitrogen, and sulfur (CHONS), whose structures, formation, and impacts are understudied. The dilution-corrected absolute ion abundance of particle-phase CHONS compounds increased with plume age by a factor of 6.4 over the first 4 hours of downwind transport, and their relative contribution to the observed functionalized

organic aerosol (OA) mixture increased from 19% to 40%. The dilution-corrected absolute ion abundance of particle-phase compounds with sulfide functional groups increased by a factor of 13 with plume age, and their relative contribution to observed OA increased from 4% to 40%. Sulfides were present in up to 75% of CHONS compounds and the increases in sulfides were accompanied by increases in ring-bound nitrogen; both increased together with CHONS prevalence. A complex mixture of intermediate- and semi-volatile gas-phase organic sulfur species was observed in emissions from the fire and depleted downwind, representing potential precursors to particle-phase CHONS compounds. These results demonstrate CHONS formation from nitrogen/oxygen-containing biomass burning emissions in the presence of reduced sulfur species. In addition, they highlight chemical pathways that may also be relevant in situations with elevated emissions of nitrogen- and sulfur-containing organic compounds from residential biomass burning and fossil fuel use (e.g. coal), respectively.

1 Introduction

Forest fires are predicted to become increasingly prevalent and severe with climate change (Abatzoglou and Williams, 2016; Barbero et al., 2015; Jolly et al., 2015). These fires are an important and uncontrolled source of gas- and particle-phase compounds to the atmosphere, including a complex mixture of gas-phase reactive organic carbon, primary organic aerosol (POA), carbon monoxide, carbon dioxide, methane, ammonia, nitrogen oxides, and black carbon (Akagi et al., 2011; Gilman et al., 2015; Hatch et al., 2015, 2018; Koss et al., 2018; Vicente et al., 2013; Yokelson et al., 2013). Many of these emitted compounds are precursors to downwind ozone and secondary organic aerosol (SOA) production (Ahern et al., 2019; Buysse et al., 2019; Gilman et al., 2015; Hennigan et al., 2011; Lim et al., 2019).

Primary and secondary pollutants from biomass burning have important effects on air quality locally, regionally, and continentally (Burgos et al., 2018; Colarco et al., 2004; Cottle et al., 2014; Dreessen et al., 2016; Forster et al., 2001; Rogers et al., 2020; Val Martín et al., 2006), and their impacts on human health and climate (e.g. via light absorbing brown and black carbon) have been well documented (Forrister et al., 2015; Jiang et al., 2019; Liu et al., 2017; Di Lorenzo et al., 2018; Reid et al., 2016; Sengupta et al., 2018; Wong et al., 2019). These health and climate effects are sensitive to the elemental and structural composition of gas- and particle-phase emissions and transformation products (Hallquist et al., 2009; Nozière et al., 2015). As a result, past studies have used online and offline mass spectrometry techniques to characterize the chemical composition of fresh and aged biomass burning emissions and have revealed a wide array of emitted hydrocarbons and oxygen-, nitrogen-, or sulfur-containing functionalized species (Ahern et al., 2019; Bertrand et al., 2018; Gilman et al., 2015; Hatch et al., 2015, 2018, 2019; Iinuma et al., 2010; Koss et al., 2018; Laskin et al., 2009; Yokelson et al., 2013). However, the emissions and chemical transformations occurring in ambient biomass burning plumes are extremely complex and despite previous measurements remain poorly understood at the molecular-level.

In this study, we used an aircraft sampling system developed to collect offline gas- and particle-phase organic compounds above a boreal forest fire. We examined the molecular-level emissions and evolution of the forest fire plume via an analysis of these offline samples using gas and liquid chromatography (GC/LC) with high resolution mass spectrometry (MS), including tandem mass spectrometry (MS/MS). This degree of detailed chemical speciation is important to advance knowledge of in-plume chemical pathways and reaction products, long-distance

transport, and fate of biomass burning products—all of which will improve modeling capabilities and our understanding of the health and environmental impacts of biomass burning.

Specifically, the goals of this study were: (1) to perform a detailed speciation of gas- and particle-phase organic compounds derived from the boreal forest fire in terms of elemental and functional group composition, to assess changes in composition at the molecular-level as the plume aged; and (2) to examine the evolution of oxygen-, nitrogen-, and sulfur-containing (CHONS) compounds. These CHONS compounds made up 19-40% of functionalized OA here and have been observed at other ambient sites (e.g. 9-11% (Ditto et al., 2018)), though little is known about their structures or formation mechanisms. Using our observations of gas-phase sulfur species, we identified possible precursors and reaction pathways involved in the formation of these CHONS compounds.

2 Materials and Methods

On June 25th, 2018, two research flights were conducted by Environment and Climate Change Canada as part of their Air Pollution research program. These flights sampled two boreal wildfire smoke plumes originating near Lac La Loche in northern Saskatchewan, Canada (Figure S1). The region is dominated by pine and spruce trees (Canada's National Forest Inventory, 2020). Gas- and particle-phase samples were collected from the National Research Council of Canada's Convair-580 research aircraft for analysis with offline high resolution mass spectrometry, alongside many other measurements (Supporting Information S1-S2). The aircraft flew the same straight-line tracks at multiple altitudes through the smoke plumes (average altitudes shown in Table S1), which when stacked created a virtual screen intercepting the plumes at each of five downwind locations (with flight design similar to those previously

reported (Li et al., 2017; Liggio et al., 2016)). Screen 1 was ~10 km from the fire with screens 2-4 following the plumes downwind, and screen 5 intercepting the plumes after they had passed over several major surface and in-situ mining oil sands facilities (Figure S1). The samples discussed here were collected across both plumes to ensure that enough mass was present to well surpass the mass spectrometer's detection limits. Based on satellite information and aircraft measurements at the start of sampling (i.e. screen 1), the fire was a low-intensity surface fire with smoldering conditions; aircraft measurements indicated a modified combustion efficiency of 0.90±0.01 for both plumes.

Combined gas- and particle-phase samples were collected onto custom adsorbent tubes packed with high-purity quartz wool, glass beads, Tenax TA, and Carbopack X (Sheu et al., 2018). Samples were collected along screens 1-4 in Figure S1 (no adsorbent tubes collected at screen 5) via an external pod mounted under the wing of the aircraft, which included remote switching between adsorbent tubes at various transect altitudes and online measurements of temperature, pressure, and flow (Supporting Information S1, Figure S2).

All adsorbent tubes were analyzed using a GERSTEL Thermal Desorber TD 3.5+ with gas chromatography (Agilent 7890B GC), atmospheric pressure chemical ionization (APCI), and quadrupole time-of-flight mass spectrometry (Agilent 6550 Q-TOF), similar to past work (Khare et al., 2019). For adsorbent tubes, the APCI was operated in positive ionization mode and the Q-TOF was operated in MS mode (i.e. TOF data collection only, hereafter "GC-APCI-MS"). Adsorbent tube data were processed primarily via a targeted approach for C_xH_y, $C_xH_yO_1$, $C_xH_yS_1$, and $C_xH_yN_1$ compounds using custom Igor Pro code (Supporting Information S2-S3).

In order to reduce losses of lower volatility gases onto upstream surfaces, particles were not explicitly filtered out at the inlet of the wing-pod sampler used for adsorbent tube collection.

For several reasons, it was concluded that the C_xH_y hydrocarbons smaller than C_{22-23} (and $C_xH_yS_1/C_xH_yO_1/C_xH_yN_1$ compounds of similar volatility) measured in the adsorbent tubes were predominantly in the gas-phase. This was based on (1) significant undersampling for particles at the wing pod inlet since the adsorbent tube sampling flow rate was a factor of ~4 lower than its corresponding isokinetic flow rate, resulting in a significant divergence of particles away from the inlet during sampling; and (2) partitioning theory, using average in-plume organic aerosol (OA) concentrations of 18-22 μg/m^3 across adsorbent tube sampling periods for screens 1-4, concurrently measured by an aerosol mass spectrometer (AMS) onboard the aircraft (see Supporting Information S1, S3, Table S2). Thus, the C_{22} and smaller C_xH_y compounds (and other compound classes of similar volatility) should have primarily been in the gas phase at equilibrium. As such, we limited the following adsorbent tube data analysis to compounds in the C_{10}-C_{25} range to focus on intermediate-volatility and semivolatile (I/SVOCs) compounds present in the gas phase. In our analyses and interpretation, the compounds included in each of these volatility ranges are defined based on fixed values of saturation mass concentrations (e.g. Donahue et al., 2011; Murphy et al., 2014) at the observed 18-22 ug/m^3 OA loadings present during adsorbent tube sampling times.

Dedicated particle-phase samples were collected on 47 mm PTFE filters (2.0 μm pore; Pall Corporation) from a sampling manifold in the aircraft cabin containing six independent anodized aluminum filter holders. The filters were sampled behind an isokinetic inlet with a size cutoff of approximately 2.5 μm. One filter sample was collected per screen for screens 1-5 shown in Figure S1.

Filter samples were extracted in methanol (Ditto et al., 2018). Samples were analyzed via liquid chromatography (Agilent 1260 LC) with electrospray ionization (ESI) and the same Q-

TOF. For filters, the ESI source was operated in both positive and negative ionization modes, and the Q-TOF was operated in both MS mode (i.e. TOF data collection, "LC-ESI-MS") and MS/MS mode (i.e. tandem mass spectral data collection, "LC-ESI-MS/MS") (Ditto et al., 2018, 2020). Filter extracts were also analyzed using GC-APCI-MS in positive ionization mode. Filter data from LC-ESI-MS, LC-ESI-MS/MS, and GC-APCI-MS were analyzed with a non-targeted approach, using Agilent Mass Hunter, SIRIUS with CSI:FingerID, and custom R code (Supporting Information S2-S3) (Ditto et al., 2018, 2020). All peaks that passed strict QA/QC (Section S3) were assigned molecular formulas, with candidate formulas limited to 20 oxygen, 3 nitrogen, and/or 1 sulfur atom(s). Hereafter, LC-ESI compound classes are discussed here without subscripts.

The particle-phase compounds observed via LC-ESI vs. GC-APCI techniques varied significantly in their oxygen, nitrogen, and sulfur content since these two chromatographic and ionization approaches are sensitive towards different types of compounds (see Section S5). As the forest fire plume aged, the complex mixture of emissions and secondary products became increasingly functionalized and thus less GC-amenable without derivatization. Therefore, we focused on LC-ESI-MS data to study these functionalized particle-phase compounds. We acknowledge that this method excludes fully-reduced hydrocarbons and fully-reduced sulfur-containing particle-phase compounds (i.e. CH and CHS (Ditto et al., 2018)) and thus these compound classes are not accounted for in the relative particle-phase distributions shown here.

For particle-phase analyses, we estimated saturation mass concentration based on the Li et al. parameterization (Li et al., 2016), then grouped compounds based on fixed volatility bins (Donahue et al., 2011; Murphy et al., 2014). Particle-phase compounds were observed across the IVOC, SVOC, LVOC, and ELVOC ranges. Particle-phase IVOCs have been observed in the

past, and despite their higher volatility, may exist in the particle-phase due to their polarity and water solubility. Additional details on these methods, including a discussion of total mass analyzed from filters/adsorbent tubes and QA/QC, are discussed in Supporting Information S1-S5, with a methods summary shown in Figure S3.

3 Results

3.1 Evolution of organic aerosol elemental composition and functionality with plume age

Our analysis of functionalized OA showed several compositional trends in the evolving boreal forest fire smoke plume (screens 1-4) and exhibited marked changes after emissions from the oil sands facilities were mixed with the forest fire plume (screen 5). Here, we focused on the forest fire plume in screens 1-4. We observed a diverse elemental composition in functionalized OA across oxygen-, nitrogen-, and/or sulfur-containing compound classes (Figure 1A-1B, Figure S5). This included oxygenates (CHO), such as common biomass burning tracers and their isomers (e.g. levoglucosan, Supporting Information S2); as well as oxygen- and nitrogen-containing compounds (CHON); oxygen- and sulfur-containing compounds (CHOS); reduced nitrogen-containing compounds (CHN); reduced nitrogen- and sulfur-containing compounds (CHNS); as well as compounds containing oxygen, nitrogen, and sulfur (CHONS).

There was a continual decrease in the relative abundance of particle-phase CHO compounds in the observed functionalized OA across screens 1-4, accompanied by a consistent relative increase in CHON and CHONS compounds (Figure 1B). Notably, the relative abundance of CHONS compounds increased from 19% to 40% of measured functionalized OA from screens 1 to 4. Trends in absolute ion abundances were also similar (note: carbon monoxide mixing ratio was used to account for dilution). This is shown in Figure 1C (inset) and Figure S5C; CHO

generally decreased from screens 1 to 4, while CHONS and CHON generally increased, suggesting that CHONS compounds were possibly formed from CHO, CHN, and/or CHON precursors in the gas- and/or particle-phases. Specifically, the dilution-corrected abundance of CHONS species increased by a factor of 6.4 from screen 1 to 4 (Figure 1C, inset). In Figure 1, we primarily presented data as relative contributions to functionalized OA to examine changes in the evolution of the complex mixture as a whole and the relationships between different compound classes and functional groups with plume age. However, dilution-corrected abundances are also important for understanding absolute formation (or depletion), and are shown for all species in Figures S5-S6.

Based on MS/MS analyses, these evolving CHO, CHN, CHON, and CHONS compounds were often comprised of variable combinations of hydroxyl and ether functional groups (e.g. primary emissions from forest fires like methoxyphenols and similar structures), as well as amine, imine, and sulfide groups, along with cyclic nitrogen structural features (consistent with past laboratory observations of biomass burning emissions (Laskin et al., 2009; Lin et al., 2018; Liu et al., 2015; Updyke et al., 2012)).

3.2 Detailed speciation of CHONS compounds in functionalized OA

While some individual CHONS species contained grouped oxygen, nitrogen, and sulfur atom moieties (e.g. sulfonamides), the majority of CHONS compounds had a combination of multiple separate oxygen-, nitrogen-, and/or sulfur-containing functional groups (Figure 2A-2B). Sulfide groups were important contributors to CHONS compounds (Figure 2B) and showed a notable increase in relative contribution to the overall functional group distribution with plume age (Figure 1C). They increased from 4% to 40% of measured compound abundance across

screens 1 to 4 (Figure 1C), which corresponded to an increase by a factor of 13 in terms of their dilution-corrected abundance (Figure 1C, inset). Their increasing relative contribution to CHONS compounds with plume evolution was even more pronounced—by screen 4, the sulfide functional group was present in 75% of detected CHONS compound abundance (Figure S7A). Here, we focused on the presence of sulfides in CHONS compounds because most of the observed particle-phase sulfides occurred as part of CHONS species (71%), while a smaller fraction occurred in CHOS (21%) or CHNS (8%) compounds (Figure 3A).

To explore possible precursors and formation pathways for these particle-phase sulfide-containing CHONS species, we used MS/MS to identify nitrogen-containing functional groups that co-occurred with sulfides. In CHONS compounds, most sulfides co-occurred with cyclic nitrogen (36% of sulfide-containing species), amine (32%), or imine features (43%) (Figure 3B). The prevalence of sulfide and cyclic nitrogen features in the measured functionalized OA increased together screen-to-screen, and increased together with the rising proportion of CHONS compounds (Figure 3C). While sulfides often co-occurred with amines or imines and while amines and imines were prevalent in all 4 screens (Figure 1C), there was no relationship between these functional groups and the increasing contribution of CHONS compounds to measured functionalized OA (Figure S7B).

The sulfide substructures observed via MS/MS often contained linear carbon chains or phenyl groups bonded to the sulfur atom (Figure 3C inset). Thus, we hypothesize that precursors with similar reduced sulfur-containing structures reacted with cyclic nitrogen-containing species to form the observed particle-phase sulfide-containing CHONS compounds (see further discussion of possible precursors in Section 3.3, and potential chemical pathways in Section 4.2).

CHONS compounds were predominantly SVOCs in screens 1-4 (i.e. 89% of CHONS ion abundance, Figure 2C, Figure S8), suggesting that these compounds were formed from higher volatility gas-phase species. In contrast, with the added influence of the oil sands facilities in screen 5, 68% of CHONS compounds were extremely low volatility organic compounds (ELVOCs), though CHONS made up only 2% of functionalized OA at screen 5.

Overall, dilution-corrected abundances of functionalized OA in each particle-phase volatility bin increased with plume age, but the relative contribution of SVOCs increased from 37% to 58% while the relative contribution of IVOCs dropped from 38% to 20%, potentially due to oxidation reactions that formed SVOCs and/or due to evaporation (Figure S9). These particle-phase IVOCs consisted predominantly of CHO, CHN, and CHON (O/N < 3) compounds, which could include possible non-sulfur containing precursors to the observed CHONS species. Fragmentation of particle-phase L/ELVOC compounds also could have contributed to some of the observed SVOC mass, but the overall increasing total abundance across all volatility bins with plume age supports the idea that these compounds were predominantly formed from more volatile precursors (e.g. I/SVOCs).

3.3 Targeted search for CHONS precursors in the gas-phase

To investigate the precursors and chemistry that could have formed the sulfide-containing CHONS species observed in the particle-phase samples, we performed a targeted search for possible gas-phase I/SVOC species in each adsorbent tube, across all C_{10}-C_{25} $C_xH_yS_1$ species with the equivalent of 0-15 double bonds and/or rings (i.e. $C_xH_{2x+2}S_1$- $C_xH_{2x-28}S_1$, Figure 4A, Figure S10). We observed a distribution of $C_xH_yS_1$ compounds and their isomers; based on the high mass resolution and high mass accuracy molecular formulas from targeted GC-APCI-MS

analysis, 27% of $C_xH_yS_1$ compounds were fully saturated (i.e. $C_xH_{2x+2}S_1$) and 25% contained the equivalent of 4-6 double bonds and/or rings (i.e. $C_xH_{2x-6}S_1$- $C_xH_{2x-10}S_1$), which included single ring aromatics. We focused on these sulfur-containing gases as candidate precursors to the observed particle-phase sulfide-containing CHONS compounds as they contained sulfur substructures with linear carbon chains or phenyl groups, similar to those observed on particle-phase CHONS compounds via MS/MS analysis (Figure 3C inset, Figures S10-S11). However, we also observed contributions from other sulfur-containing structures (e.g. with the equivalent of 1-3 double bonds and/or rings, Figure 4A), which could also have been precursor species.

The observed gas-phase C_{10}-C_{25} $C_xH_yS_1$ compounds were present in gas-phase emissions from the fire and likely also evaporated from primary OA during early plume dilution. Gas-phase C_{10}-C_{25} $C_xH_yS_1$ concentrations increased relative to carbon monoxide from screen 1 to 2, then steadily decreased with plume age (Figure 4B, Figure S12A). This suggests the gas-phase emission and/or evaporation of $C_xH_yS_1$ compounds from OA between screens 1 and 2, and subsequent participation in plume chemistry from screens 2 to 4.

Similar OA evaporation with plume dilution has been observed in many past studies (Ahern et al., 2019; Garofalo et al., 2019; Hennigan et al., 2011; Lim et al., 2019). To better understand the dynamics of these sulfur-containing compounds and their possible particle-phase origin, we compared their concentrations to those of C_{10}-C_{25} aliphatic and aromatic C_xH_y and $C_xH_yO_1$ species from a similar targeted search of adsorbent tube gas-phase compounds. Overall, C_xH_y and $C_xH_yO_1$ compound classes dominated the observed C_{10}-C_{25} compounds (Figure 4B, Figure S12B), with 61% C_xH_y, 36% $C_xH_yO_1$, and just 3% $C_xH_yS_1$ on average. C_xH_y and $C_xH_yO_1$ concentrations generally increased with plume age (Figure 4B) and included many known compound types (e.g. monoterpenes, aromatics, hydroxyls, carbonyls (Akagi et al., 2011;

Andreae, 2019; Gilman et al., 2015; Hatch et al., 2015, 2019; Koss et al., 2018)). This suggests the direct emission of these gas-phase compound classes from the fire (observed at screen 1) along with the evaporation of semivolatile particle-phase emissions as the plume evolved, and formation of $C_xH_yO_1$ via C_xH_y oxidation. AMS measurements of total OA concentrations provided supporting evidence of OA evaporation; the ratio of AMS OA concentration to CO decreased by 7% from screen 1 to 2 (corresponding to an AMS OA/CO ratio of -0.0044 or a decrease in OA concentrations of -2.3 μg/m^3), while the ratio of total gas-phase C_xH_y, $C_xH_yO_1$, and $C_xH_yS_1$ concentration to CO increased by 55% (corresponding to a total gas-phase concentration/CO ratio of 0.022 or an increase in gas-phase concentration of 7.0 μg/m^3, with changes summarized in Table S3). While not the focus of the analytical approaches applied in this study, to further substantiate the observation of OA evaporation, we performed the same targeted analysis of C_{10}-C_{25} C_xH_y, $C_xH_yO_1$, and $C_xH_yS_1$ compounds in the particle-phase filter sample extracts analyzed via GC-APCI-MS. We observed a similar decrease in concentration from screen 1 to 2. However, these filter measurements (even with APCI ionization) were not geared towards C_xH_y and $C_xH_yS_1$ speciation due to possible solubility limitations in the extraction solvent (Supporting Information S4). Direct thermal desorption of quartz filters with GC-APCI analysis would be better suited for these C_xH_y and $C_xH_yS_1$ measurements (as performed in this study with adsorbent tubes).

As discussed in *Materials and Methods*, the observed compounds with volatilities below that of ~C_{22}-C_{23} hydrocarbons existed primarily in the gas-phase (Table S2), while larger compounds favored the particle-phase (with a smaller fraction in the gas-phase at equilibrium). The presence of gas-phase compounds across this I/SVOC range (e.g. Figures S10, S13) further corroborates the possibility of contributions from both direct gas-phase emissions and from

evaporation of particle-phase emissions (Supporting Information S3). In contrast to C_xH_y concentrations, $C_xH_yS_1$ concentrations dropped markedly after screen 2 despite similarities in the volatility distribution of C_xH_y and $C_xH_yS_1$ I/SVOC mixtures (Figure 4A, Figures S10 and S13). This difference across screens shows that the observed $C_xH_yS_1$ I/SVOCs were removed (e.g. via chemical reactions) more quickly than C_xH_y (Figure 4B), thus supporting their potential contribution to CHONS formation.

In addition to the C_{10}-C_{25} $C_xH_yS_1$ compounds measured in the adsorbent tubes, smaller sulfur-containing compounds could have also acted as CHONS precursors, like those identified by the onboard proton transfer reaction-mass spectrometer (PTR-ToF-MS). While dimethyl sulfide (DMS, previously observed in biomass burning smoke (Andreae, 2019)) was often below the instrument's limit of detection, both dimethyl and diethyl sulfide showed good correlation with acetonitrile (a well-known biomass burning product (Andreae, 2019)) in the smoke plume during screen 1 ($r \sim 0.95$, Figure S12C). This suggests that these compounds were co-emitted by the fire.

4 Discussion

4.1 Investigating possible origins of gas-phase sulfur compounds

The gas-phase sulfur-containing compounds observed in the plume were emitted from the smoldering fire. However, their origins are uncertain, since the broader range of sulfur species found here (Figure 4A, Figures S10-11) has not been previously reported; many of the compounds in the complex mixture of sulfur-containing compounds discussed in this work were outside the detection range of previously employed methods (Hatch et al., 2015; Khare et al., 2019; Koss et al., 2018; Sekimoto et al., 2018). Here, we explore two potential origins of these

gas-phase sulfur-containing precursors to the observed particle-phase CHONS compounds: the biomass fuel itself and the deposition of sulfur species from anthropogenic/industrial operations.

Fuel: In past studies, emissions of sulfur-containing organic compounds were typically minor compared to oxygen- or nitrogen-containing compounds, and the relative balance of oxygen-, nitrogen-, or sulfur-containing compound emissions was typically proportional to fuel content (Hatch et al., 2015; Ward, 1990). The estimated N:S ratio for boreal forest fuel near the fire was ~10:1 (Huang and Schoenau, 1996), which was similar to the average N:S ratio from a non-targeted search for nitrogen- and sulfur-containing I/SVOCs from the adsorbent tube samples in this study of (8.1 ± 4.8):1. Sulfur is an essential nutrient in plants, and can be taken up from soil (as sulfate) or from the atmosphere via deposition (as SO_2 and sulfate) (Aas et al., 2019; Gahan and Schmalenberger, 2014; Leustek, 2002). Both SO_2 and sulfate are metabolized in plants to yield a variety of compounds critical to plant functions including cysteine and a range of other sulfur- (as well as oxygen- and nitrogen-) containing compounds (Leustek, 2002). In addition, disulfide bonds contribute to plant protein structure, and these bonds can cleave and form thiols (Gahan and Schmalenberger, 2014; Leustek, 2002; Onda, 2013). Sulfur-containing compounds like these may have been emitted during the fire, along with other known sulfur products from boreal fuels (e.g. DMS, thiophenes (Akagi et al., 2011; Hatch et al., 2015; Koss et al., 2018; Landis et al., 2018)).

Deposition: While sulfur can be naturally occurring, it is also associated with anthropogenic activities (e.g. transportation, power generation, industry, etc.). A portion of the sulfur in the forest fire emissions could have originated from sulfur deposited via such anthropogenic activities. The closest large anthropogenic sulfur source to the fire location was the oil sands mining region north of Fort McMurray, Alberta, which was approximately 150 km

away and which contains known SO_2 emitters (Liggio et al., 2017; McLinden et al., 2016). Regional concentrations of SO_2 or other sulfur species from these nearby industrial activities could have led to accumulated deposition of inorganic and/or organic sulfur compounds over time, though it is uncertain how much of this deposited sulfur would have been taken up and transformed by vegetation due to sulfur uptake and assimilation regulatory pathways in plants (Davidian and Kopriva, 2010). This possible accumulated deposition may have acted as a reservoir of sulfur to be emitted during fires via the re-volatilization of deposited compounds, in addition to the evaporation of typical sulfur metabolites or the formation of sulfur-containing combustion by-products. This hypothesis is consistent with recent deposition measurement and modeling results for the region, which indicated that sulfur deposition from the oil sands operations potentially impacted areas downwind, including the region where this fire occurred (Makar et al., 2018).

Interestingly, lichen and spruce trees, which are prominent in the region of the fire discussed here, have been reported to accumulate sulfur from SO_2 in regions near large industrial SO_2 sources (Meng et al., 1995; Nyborg et al., 1991). Also, past studies have reported enhancements in sulfate (as well as nitrate/ammonium) aerosols coming from biomass burning in areas with urban influence (Fenn et al., 2015; Hecobian et al., 2011; Hegg et al., 1987). Inorganic aerosol components from both urban (e.g. Edmonton, Alberta) and industrial (e.g. oil sands) sources could deposit in the area surrounding the emissions source along with an organic phase, which we postulate could contain a range of sulfur-containing species including the $C_xH_yS_1$ compounds shown here. These deposited inorganic and organic species may have re-volatilized during the fire. However, further work is needed to disentangle the contribution of natural vs. anthropogenic sulfur to biomass burning emissions in the region. Also, we note that

the fire was ~1 hour old at the time of sampling, so the recent application of fire suppressants was unlikely to contribute to the species observed.

4.2 Potential reaction pathways leading to sulfides in CHONS from sulfur precursors

A number of potential reactions involving sulfur-containing precursors, often thiols (R-SH), may have contributed to the formation of the observed sulfide functional groups in particle-phase CHONS compounds (Figure S14). On average, our gas-phase measurements were comprised of 27% fully saturated sulfur-containing hydrocarbons (i.e. $C_xH_{2x+2}S_1$, Figures S10-11). It is likely that some fraction of the sulfur compounds observed in the gas-phase adsorbent tube measurements (e.g. the compounds identified as $C_xH_{2x+2}S_1$) and in PTR-ToF-MS measurements (e.g. dimethyl sulfide, diethyl sulfide) were thiols, but the distinction between sulfide vs. thiol isomers was challenging with these methods without specific internal standards.

In some of the following possible reactions, a thiol interacts with a non-sulfur precursor to yield a sulfide-containing compound. The non-sulfur precursor (in the gas- or particle-phase) may have contained O and N atoms, thus yielding a CHONS compound immediately after participating in one of the proposed reactions. Alternatively, the newly formed sulfide-containing compound may have undergone subsequent, separate reactions with oxygen- and/or nitrogen-containing species (in the gas- or particle-phase) to form the observed sulfide-containing CHONS species. Here, we focused on possible reactions that could have contributed the sulfide group to these oxygen- and/or nitrogen-containing compounds (known emissions from forest fires, as discussed above). Earlier, we postulated that because most of the observed particle-phase CHONS compounds were SVOCs, these compounds were predominantly formed by reactions with more volatile gas-phase compounds. However, it is uncertain whether these

sulfide-forming and CHONS-forming reactions all occurred in the gas-phase with subsequent partitioning to the particle-phase, heterogeneously, or in a combination of separate gas- and particle-phase chemistry. We suggest some possible sulfide-forming reactions here, yet we note that these proposed reactions are likely not comprehensive. Further work to elucidate the chemistry driving this sulfide and CHONS formation is needed.

Some possible reactions include: (1) thiol-ene reactions, where a thiol reacts with an alkene (or alkyne), which can form carbon-sulfur bonds (Lowe, 2010). Alkenes are known to be prominent in emissions from boreal fires (Gilman et al., 2015; Hatch et al., 2015), and we observed similar structures in our gas-phase samples that likely included alkenes, cyclic alkanes, and/or monoterpenes (Figure S13). (2) Thiol reactions with carbonyls, which can form hemithioacetals that subsequently dehydrate in the atmosphere to yield sulfides (Jencks and Lienhard, 1966). This reaction is similar to the formation of enamines from carbonyls and dimethyl amine via the formation and subsequent dehydration of a carbinolamine, which has been shown to occur in ambient conditions (Duporté et al., 2016, 2017). (3) Thiol reactions with alcohols, which can form sulfides; these reaction rates are low in the absence of catalysts and require relatively high temperature to occur (i.e. 200-450°C (Mashkina, 1991), temperatures that are relevant very close to the fire but unlikely in the cooled plume). (4) Another possibility is that a radical intermediate product formed during atmospheric oxidation of DMS (e.g. the methylthiomethyl radical ($CH_3SCH_2^{\bullet}$) from $OH^{\bullet}$-driven hydrogen abstraction of DMS (Barnes et al., 2006)) interacted with CHN and CHON precursors to yield the observed sulfide-containing CHONS products. However, the concentrations of the methylthiomethyl radical and similar radicals from other small sulfide precursors would likely be lower than those of other major

drivers of in-plume radical chemistry (e.g. O_2, NO_x, etc.), thus making this reaction pathway less likely to contribute.

Based on our observations of these sulfide-containing products across flight screens, the overall timescale for these sulfide-forming reactions was likely approximately 1 hour (or less). For the literature reactions referenced above, reaction timescales ranged from minutes to hours in laboratory experiments, but extrapolation to rates in an ambient wildfire plume is uncertain. Specifically, it is challenging to compare to predicted timescales for the proposed reactions without knowing the exact structure/identities of the reactants or the possible role of other key modifying factors in the plume (e.g. aerosol pH, presence of water).

5 Implications and Conclusions

In this work, we performed the first high resolution tandem mass spectrometry analysis of an evolving plume from a smoldering boreal forest fire. The results show clear evidence of gas-phase sulfur-containing emissions from the fire, and an increasing contribution from particle-phase CHONS compounds with sulfide functional groups as the plume evolved. Together, these results suggest the emission of gas-phase sulfur-containing compounds from the fire and subsequent gas- and/or particle-phase chemistry that produced multifunctional sulfide-containing CHONS compounds.

Sulfide functional groups in ambient air have been reported at a range of U.S. locations from urban inland (1-7% sulfides), urban coastal (5-12% sulfides), and remote forested (7% sulfides), and on average, sulfides comprised 28% of sulfur-containing functional groups at these sites (Ditto et al., 2020). However, in past work, 53% of these sulfides were present in CHOS compounds, while 34% were CHONS, and 13% were CHNS (in contrast to 21%, 71%, and 8%

in this study, respectively). Notably, at a Northeastern U.S. coastal site where there were several pollution events linked to long distance transport of biomass burning smoke during field sampling (Rogers et al., 2020), 70-90% of sulfides were present in CHONS compounds (Ditto et al., 2020), similar to the compound class distribution of sulfides discussed here (Figure 3A).

These results, along with past observations, highlight that this type of chemistry and these types of reaction products may be relevant to other regions where concentrations of nitrogen and sulfur-containing precursors are high, such as in developing regions, emerging economies, or megacities where residential biomass burning is common and coincident with extensive use of sulfur-containing fossil fuels (e.g. coal). CHONS compounds have been reported in similar regions in past studies (Lin et al., 2012; Pan et al., 2013; Song et al., 2019; Wang et al., 2017a, 2016, 2017b). Their formation is potentially important since the presence of sulfur, oxygen, and nitrogen atoms in organic compounds can affect particle phase state (e.g. solid, semi-solid, liquid), and mixing state (e.g. well-mixed, phase-separated) (DeRieux et al., 2018; Ditto et al., 2019; Van Krevelen and Te Nijenhuis, 2009). These physical properties may influence particles' chemical reactivity and overall persistence in the atmosphere, all of which contribute to the health and environmental impacts that communities and ecosystems experience from OA exposure. Future work to identify prominent functional groups in CHONS species in regions with high CHONS concentrations will help elucidate the formation chemistry of these functionalized compounds and understand and mitigate their associated impacts.

Acknowledgments

The authors acknowledge GERSTEL for their collaboration with the TDU 3.5+ used to run the GC-APCI adsorbent tubes and filters discussed in this study. We thank Environment and Climate Change Canada and National Research Council technical teams for their help in the construction and maintenance of cartridge sampling systems, specifically Tak Chan (Environment and Climate Change Canada) for help collecting samples. We also thank Jo Machesky (Yale) for help running adsorbent tube samples, Joe Lybik (Yale) for help packing adsorbent tubes, and Daniel Thompson (Natural Resources Canada) for informative discussion. J.C.D., M.H., T.H-M., and D.R.G. acknowledge support from National Science Foundation grant AWD0001666. We also acknowledge funding from the Air Pollution (AP) program of Environment and Climate Change Canada. The flights discussed in this study were embedded within a 2018 oil sands monitoring intensive campaign, and the oil sands monitoring program is acknowledged for enabling the flights.

Author Contributions

J.C.D. ran samples, processed filter data, compiled and interpreted results. M.H. processed adsorbent tube data. T.H-M. contributed to MS/MS analysis. S.G.M., K.H., J.L., and D.R.G. collaborated on data interpretation. K.H. collected and processed AMS data. A.L. collected and processed PTR-ToF-MS data. S.-M.L. designed the aircraft adsorbent tube collection system. P.L. and J.J.B.W. implemented the wing pod design. P.L. prepared the wing pods for collection and J.J.B.W. and J.L. collected the adsorbent tube samples. M.J.W. and J.L. designed the filter collection system. M.J.W. and K.H collected filter samples. S.-M.L., K.H., and J.L. designed the aircraft sampling study. J.C.D. and D.R.G. wrote the manuscript, with input from all co-authors.

Competing Interests

The authors declare that they have no conflicts of interest.

Code and Data Availability

Code and data are available upon request.

References

Aas, W., Mortier, A., Bowersox, V., Cherian, R., Faluvegi, G., Fagerli, H., Hand, J., Klimont, Z., Galy-Lacaux, C., Lehmann, C. M. B., Myhre, C. L., Myhre, G., Olivié, D., Sato, K., Quaas, J., Rao, P. S. P., Schulz, M., Shindell, D., Skeie, R. B., Stein, A., Takemura, T., Tsyro, S., Vet, R. and Xu, X.: Global and regional trends of atmospheric sulfur, Sci. Rep., 9(1), 1–11, doi:10.1038/s41598-018-37304-0, 2019.

Abatzoglou, J. T. and Williams, A. P.: Impact of anthropogenic climate change on wildfire across western US forests, Proc. Natl. Acad. Sci. U. S. A., 113(42), 11770–11775, doi:10.1073/pnas.1607171113, 2016.

Ahern, A. T., Robinson, E. S., Tkacik, D. S., Saleh, R., Hatch, L. E., Barsanti, K. C., Stockwell, C. E., Yokelson, R. J., Presto, A. A., Robinson, A. L., Sullivan, R. C. and Donahue, N. M.: Production of Secondary Organic Aerosol During Aging of Biomass Burning Smoke From Fresh Fuels and Its Relationship to VOC Precursors, J. Geophys. Res. Atmos., 124(6), 3583–3606, doi:10.1029/2018JD029068, 2019.

Akagi, S. K., Yokelson, R. J., Wiedinmyer, C., Alvarado, M. J., Reid, J. S., Karl, T., Crounse, J. D. and Wennberg, P. O.: Emission factors for open and domestic biomass burning for use in atmospheric models, Atmos. Chem. Phys., 11(9), 4039–4072, doi:10.5194/acp-11-

4039-2011, 2011.

Andreae, M. O.: Emission of trace gases and aerosols from biomass burning – An updated assessment, Atmos. Chem. Phys., 1–27, doi:10.5194/acp-2019-303, 2019.

Canada's National Forest Inventory, [online] Available from: https://nfi.nfis.org/en/ (Accessed 18 February 2020), 2020.

Barbero, R., Abatzoglou, J. T., Larkin, N. K., Kolden, C. A. and Stocks, B.: Climate change presents increased potential for very large fires in the contiguous United States, Int. J. Wildl. Fire, 24(7), 892–899, doi:10.1071/WF15083, 2015.

Barnes, I., Hjorth, J. and Mihalapoulos, N.: Dimethyl sulfide and dimethyl sulfoxide and their oxidation in the atmosphere, Chem. Rev., 106(3), 940–975, doi:10.1021/cr020529+, 2006.

Bertrand, A., Stefenelli, G., Jen, C. N., Pieber, S. M., Bruns, E. A., Ni, H., Temime-Roussel, B., Slowik, J. G., Goldstein, A. H., Haddad, I. El, Baltensperger, U., Prévôt, A. S. H., Wortham, H. and Marchand, N.: Evolution of the chemical fingerprint of biomass burning organic aerosol during aging, Atmos. Chem. Phys., 18(10), 7607–7624, doi:10.5194/acp-18-7607-2018, 2018.

Burgos, M. A., Mateos, D., Cachorro, V. E., Toledano, C., de Frutos, A. M., Calle, A., Herguedas, A. and Marcos, J. L.: An analysis of high fine aerosol loading episodes in north-central Spain in the summer 2013 - Impact of Canadian biomass burning episode and local emissions, Atmos. Environ., doi:10.1016/j.atmosenv.2018.04.024, 2018.

Buysse, C. E., Kaulfus, A., Nair, U. and Jaffe, D. A.: Relationships between Particulate Matter, Ozone, and Nitrogen Oxides during Urban Smoke Events in the Western US, Environ. Sci. Technol., 53(21), 12519–12528, doi:10.1021/acs.est.9b05241, 2019.

Colarco, P. R., Schoeberl, M. R., Doddridge, B. G., Marufu, L. T., Torres, O. and Welton, E. J.: Transport of smoke from Canadian forest fires to the surface near Washington, D.C.: Injection height, entrainment, and optical properties, J. Geophys. Res. D Atmos., 109(6), 1–12, doi:10.1029/2003JD004248, 2004.

Cottle, P., Strawbridge, K. and McKendry, I.: Long-range transport of Siberian wildfire smoke to British Columbia: Lidar observations and air quality impacts, Atmos. Environ., doi:10.1016/j.atmosenv.2014.03.005, 2014.

Davidian, J.-C. and Kopriva, S.: Regulation of Sulfate Uptake and Assimilation—the Same or Not the Same?, Mol. Plant, 3(2), 314–325, doi:10.1093/MP/SSQ001, 2010.

DeRieux, W.-S. W., Li, Y., Lin, P., Laskin, J., Laskin, A., Bertram, A. K., Nizkorodov, S. A. and Shiraiwa, M.: Predicting the glass transition temperature and viscosity of secondary organic material using molecular composition, Atmos. Chem. Phys., 18(9), 6331–6351, doi:10.5194/acp-18-6331-2018, 2018.

Ditto, J. C., Barnes, E. B., Khare, P., Takeuchi, M., Joo, T., Bui, A. A. T., Lee-Taylor, J., Eris, G., Chen, Y., Aumont, B., Jimenez, J. L., Ng, N. L., Griffin, R. J. and Gentner, D. R.: An omnipresent diversity and variability in the chemical composition of atmospheric functionalized organic aerosol, Commun. Chem., 1(1), 75, doi:10.1038/s42004-018-0074-3, 2018.

Ditto, J. C., Joo, T., Khare, P., Sheu, R., Takeuchi, M., Chen, Y., Xu, W., Bui, A. A. T., Sun, Y., Ng, N. L. and Gentner, D. R.: Effects of Molecular-Level Compositional Variability in Organic Aerosol on Phase State and Thermodynamic Mixing Behavior, Environ. Sci. Technol., 53(22), 13009–13018, doi:10.1021/acs.est.9b02664, 2019.

Ditto, J. C., Joo, T., Slade, J. H., Shepson, P. B., Ng, N. L. and Gentner, D. R.: Nontargeted

Tandem Mass Spectrometry Analysis Reveals Diversity and Variability in Aerosol Functional Groups across Multiple Sites, Seasons, and Times of Day, Environ. Sci. Technol. Lett., 7(2), 60–69, doi:10.1021/acs.estlett.9b00702, 2020.

Donahue, N. M., Epstein, S. A., Pandis, S. N. and Robinson, A. L.: A two-dimensional volatility basis set: 1. organic-aerosol mixing thermodynamics, Atmos. Chem. Phys., 11(7), 3303–3318, doi:10.5194/acp-11-3303-2011, 2011.

Dreessen, J., Sullivan, J. and Delgado, R.: Observations and impacts of transported Canadian wildfire smoke on ozone and aerosol air quality in the Maryland region on June 9–12, 2015, J. Air Waste Manag. Assoc., 66(9), 842–862, doi:10.1080/10962247.2016.1161674, 2016.

Duporté, G., Parshintsev, J., Barreira, L. M. F., Hartonen, K., Kulmala, M. and Riekkola, M. L.: Nitrogen-Containing Low Volatile Compounds from Pinonaldehyde-Dimethylamine Reaction in the Atmosphere: A Laboratory and Field Study, Environ. Sci. Technol., 50(9), 4693–4700, doi:10.1021/acs.est.6b00270, 2016.

Duporté, G., Riva, M., Parshintsev, J., Heikkinen, E., Barreira, L. M. F., Myllys, N., Heikkinen, L., Hartonen, K., Kulmala, M., Ehn, M. and Riekkola, M. L.: Chemical Characterization of Gas- and Particle-Phase Products from the Ozonolysis of α-Pinene in the Presence of Dimethylamine, Environ. Sci. Technol., 51(10), 5602–5610, doi:10.1021/acs.est.6b06231, 2017.

Fenn, M. E., Bytnerowicz, A., Schilling, S. L. and Ross, C. S.: Atmospheric deposition of nitrogen, sulfur and base cations in jack pine stands in the Athabasca Oil Sands Region, Alberta, Canada, Environ. Pollut., 196, 497–510, doi:10.1016/j.envpol.2014.08.023, 2015.

573 Forrister, H., Liu, J., Scheuer, E., Dibb, J., Ziemba, L., Thornhill, K. L., Anderson, B., Diskin,
574 G., Perring, A. E., Schwarz, J. P., Campuzano-Jost, P., Day, D. A., Palm, B. P., Jimenez,
575 J. L., Nenes, A. and Weber, R. J.: Evolution of brown carbon in wildfire plumes,
576 Geophys. Res. Lett., 42, 4623–4630, 2015.
577 Forster, C., Wandinger, U., Wotawa, G., James, P., Mattis, I., Althausen, D., Simmonds, P.,
578 O'Doherty, S., Jennings, S. G., Kleefeld, C., Schneider, J., Trickl, T., Kreipl, S., Jäger, H.
579 and Stohl, A.: Transport of boreal forest fire emissions from Canada to Europe, J.
580 Geophys. Res. Atmos., 106(D19), 22887–22906, doi:10.1029/2001JD900115, 2001.
581 Gahan, J. and Schmalenberger, A.: The role of bacteria and mycorrhiza in plant sulfur supply,
582 Front. Plant Sci., 5(DEC), 1–7, doi:10.3389/fpls.2014.00723, 2014.
583 Garofalo, L. A., Pothier, M. A., Levin, E. J. T., Campos, T., Kreidenweis, S. M. and Farmer, D.
584 K.: Emission and Evolution of Submicron Organic Aerosol in Smoke from Wildfires in
585 the Western United States, ACS Earth Sp. Chem., 3(7), 1237–1247,
586 doi:10.1021/acsearthspacechem.9b00125, 2019.
587 Gilman, J. B., Lerner, B. M., Kuster, W. C., Goldan, P. D., Warneke, C., Veres, P. R., Roberts, J.
588 M., De Gouw, J. A., Burling, I. R. and Yokelson, R. J.: Biomass burning emissions and
589 potential air quality impacts of volatile organic compounds and other trace gases from
590 fuels common in the US, Atmos. Chem. Phys., 15(24), 13915–13938, doi:10.5194/acp-
591 15-13915-2015, 2015.
592 Hallquist, M., Wenger, J. C., Baltensperger, U., Rudich, Y., Simpson, D., Claeys, M., Dommen,
593 J., Donahue, N. M., George, C., Goldstein, A. H., Hamilton, J. F., Herrmann, H.,
594 Hoffmann, T., Iinuma, Y., Jang, M., Jenkin, M. E., Jimenez, J. L., Kiendler-Scharr, A.,
595 Maenhaut, W., McFiggans, G., Mentel, T. F., Monod, A., Prevot, A. S. H., Seinfeld, J.

H., Surratt, J. D., Szmigielski, R. and Wildt, J.: The formation, properties and impact of secondary organic aerosol: current and emerging issues, Atmos. Chem. Phys., 9(14), 5155–5236, doi:10.5194/acp-9-5155-2009, 2009.

Hatch, L. E., Luo, W., Pankow, J. F., Yokelson, R. J., Stockwell, C. E. and Barsanti, K. C.: Identification and quantification of gaseous organic compounds emitted from biomass burning using two-dimensional gas chromatography-time-of-flight mass spectrometry, Atmos. Chem. Phys., 15(4), 1865–1899, doi:10.5194/acp-15-1865-2015, 2015.

Hatch, L. E., Rivas-Ubach, A., Jen, C. N., Lipton, M., Goldstein, A. H. and Barsanti, K. C.: Measurements of I/SVOCs in biomass-burning smoke using solid-phase extraction disks and two-dimensional gas chromatography, Atmos. Chem. Phys., 18(24), 17801–17817, doi:10.5194/acp-18-17801-2018, 2018.

Hatch, L. E., Jen, C. N., Kreisberg, N. M., Selimovic, V., Yokelson, R. J., Stamatis, C., York, R. A., Foster, D., Stephens, S. L., Goldstein, A. H. and Barsanti, K. C.: Highly Speciated Measurements of Terpenoids Emitted from Laboratory and Mixed-Conifer Forest Prescribed Fires, Environ. Sci. Technol., 53(16), 9418–9428, doi:10.1021/acs.est.9b02612, 2019.

Hecobian, A., Liu, Z., Hennigan, C. J., Huey, L. G., Jimenez, J. L., Cubison, M. J., Vay, S., Diskin, G. S., Sachse, G. W., Wisthaler, A., Mikoviny, T., Weinheimer, A. J., Liao, J., Knapp, D. J., Wennberg, P. O., Kürten, A., Crounse, J. D., St. Clair, J., Wang, Y. and Weber, R. J.: Comparison of chemical characteristics of 495 biomass burning plumes intercepted by the NASA DC-8 aircraft during the ARCTAS/CARB-2008 field campaign, Atmos. Chem. Phys., 11(24), 13325–13337, doi:10.5194/acp-11-13325-2011, 2011.

Hegg, D. A., Radke, L. F., Hobbs, P. V. and Brock, C. A.: Nitrogen and Sulfur Emissions From The Burning of Forest Products Near Large Urban Areas, J. Geophys. Res., 92, 701–714, 1987.

Hennigan, C. J., Miracolo, M. A., Engelhart, G. J., May, A. A., Presto, A. A., Lee, T., Sullivan, A. P., McMeeking, G. R., Coe, H., Wold, C. E., Hao, W. M., Gilman, J. B., Kuster, W. C., De Gouw, J., Schichtel, B. A., Collett, J. L., Kreidenweis, S. M. and Robinson, A. L.: Chemical and physical transformations of organic aerosol from the photo-oxidation of open biomass burning emissions in an environmental chamber, Atmos. Chem. Phys., 11(15), 7669–7686, doi:10.5194/acp-11-7669-2011, 2011.

Huang, W. Z. and Schoenau, J. J.: Forms, amounts and distribution of carbon, nitrogen, phosphorus and sulfur in a boreal aspen forest soil, Can. J. Soil Sci., 76(3), 373–385, doi:10.4141/cjss96-045, 1996.

Iinuma, Y., Böge, O. and Herrmann, H.: Methyl-nitrocatechols: Atmospheric tracer compounds for biomass burning secondary organic aerosols, Environ. Sci. Technol., 44(22), 8453–8459, doi:10.1021/es102938a, 2010.

Jencks, W. P. and Lienhard, G. E.: Thiol Addition to the Carbonyl Group. Equilibria and Kinetics, J. Am. Chem. Soc., 88(17), 3982–3995, doi:10.1021/ja00969a017, 1966.

Jiang, H., Frie, A. L., Lavi, A., Chen, J. Y., Zhang, H., Bahreini, R. and Lin, Y. H.: Brown Carbon Formation from Nighttime Chemistry of Unsaturated Heterocyclic Volatile Organic Compounds, Environ. Sci. Technol. Lett., 6(3), 184–190, doi:10.1021/acs.estlett.9b00017, 2019.

Jolly, W. M., Cochrane, M. A., Freeborn, P. H., Holden, Z. A., Brown, T. J., Williamson, G. J. and Bowman, D. M. J. S.: Climate-induced variations in global wildfire danger from

1979 to 2013, Nat. Commun., 6(May), 1–11, doi:10.1038/ncomms8537, 2015.

Khare, P., Marcotte, A., Sheu, R., Walsh, A. N., Ditto, J. C. and Gentner, D. R.: Advances in offline approaches for trace measurements of complex organic compound mixtures via soft ionization and high-resolution tandem mass spectrometry, J. Chromatogr. A, 1598, 163–174, doi:10.1016/j.chroma.2019.03.037, 2019.

Koss, A. R., Sekimoto, K., Gilman, J. B., Selimovic, V., Coggon, M. M., Zarzana, K. J., Yuan, B., Lerner, B. M., Brown, S. S., Jimenez, J. L., Krechmer, J., Roberts, J. M., Warneke, C., Yokelson, R. J. and De Gouw, J.: Non-methane organic gas emissions from biomass burning: Identification, quantification, and emission factors from PTR-ToF during the FIREX 2016 laboratory experiment, Atmos. Chem. Phys., 18(5), 3299–3319, doi:10.5194/acp-18-3299-2018, 2018.

Van Krevelen, D. W. and Te Nijenhuis, K.: Properties of Polymers, 4th ed., Elsevier, Amsterdam., 2009.

Landis, M. S., Edgerton, E. S., White, E. M., Wentworth, G. R., Sullivan, A. P. and Dillner, A. M.: The impact of the 2016 Fort McMurray Horse River Wildfire on ambient air pollution levels in the Athabasca Oil Sands Region, Alberta, Canada, Sci. Total Environ., 618, 1665–1676, doi:10.1016/j.scitotenv.2017.10.008, 2018.

Laskin, A., Smith, J. S. and Laskin, J.: Molecular Characterization of Nitrogen-Containing Organic Compounds in Biomass Burning Aerosols Using High-Resolution Mass Spectrometry, Environ. Sci. Technol., 43(10), 3764–3771, doi:10.1021/es803456n, 2009.

Leustek, T.: Sulfate Metabolism, Arab. B., 1(e0017), 1–16, doi:10.1199/tab.0017, 2002.

Li, S. M., Leithead, A., Moussa, S. G., Liggio, J., Moran, M. D., Wang, D., Hayden, K., Darlington, A., Gordon, M., Staebler, R., Makar, P. A., Stroud, C. A., McLaren, R., Liu,

665 P. S. K., O'Brien, J., Mittermeier, R. L., Zhang, J., Marson, G., Cober, S. G., Wolde, M.
666 and Wentzell, J. J. B.: Differences between measured and reported volatile organic
667 compound emissions from oil sands facilities in Alberta, Canada, Proc. Natl. Acad. Sci.
668 U. S. A., 114(19), E3756–E3765, doi:10.1073/pnas.1617862114, 2017.
669 Li, Y., Pöschl, U. and Shiraiwa, M.: Molecular corridors and parameterizations of volatility in
670 the chemical evolution of organic aerosols, Atmos. Chem. Phys., 16(5), 3327–3344,
671 doi:10.5194/acp-16-3327-2016, 2016.
672 Liggio, J., Li, S.-M., Hayden, K., Taha, Y. M., Stroud, C., Darlington, A., Drollette, B. D.,
673 Gordon, M., Lee, P., Liu, P., Leithead, A., Moussa, S. G., Wang, D., OBrien, J.,
674 Mittermeier, R. L., Brook, J. R., Lu, G., Staebler, R. M., Han, Y., Tokarek, T. W.,
675 Osthoff, H. D., Makar, P. A., Zhang, J., Plata, D. L. and Gentner, D. R.: Oil sands
676 operations as a large source of secondary organic aerosols, Nature, 534,
677 doi:10.1038/nature17646, 2016.
678 Liggio, J., Moussa, S. G., Wentzell, J., Darlington, A., Liu, P., Leithead, A., Hayden, K., OBrien,
679 J., Mittermeier, R. L., Staebler, R., Wolde, M. and Li, S. M.: Understanding the primary
680 emissions and secondary formation of gaseous organic acids in the oil sands region of
681 Alberta, Canada, Atmos. Chem. Phys., 17(13), 8411–8427, doi:10.5194/acp-17-8411-
682 2017, 2017.
683 Lim, C. Y., Hagan, D. H., Coggon, M. M., Koss, A. R., Sekimoto, K., De Gouw, J., Warneke,
684 C., Cappa, C. D. and Kroll, J. H.: Secondary organic aerosol formation from the
685 laboratory oxidation of biomass burning emissions, Atmos. Chem. Phys., 19(19), 12797–
686 12809, doi:10.5194/acp-19-12797-2019, 2019.
687 Lin, P., Yu, J. Z., Engling, G. and Kalberer, M.: Organosulfates in humic-like substance fraction

isolated from aerosols at seven locations in East Asia: A study by ultra-high-resolution mass spectrometry, Environ. Sci. Technol., 46(24), 13118–13127, doi:10.1021/es303570v, 2012.

Lin, P., Fleming, L. T., Nizkorodov, S. A., Laskin, J. and Laskin, A.: Comprehensive Molecular Characterization of Atmospheric Brown Carbon by High Resolution Mass Spectrometry with Electrospray and Atmospheric Pressure Photoionization, Anal. Chem., 90(21), 12493–12502, doi:10.1021/acs.analchem.8b02177, 2018.

Liu, J. C., Wilson, A., Mickley, L. J., Dominici, F., Ebisu, K., Wang, Y., Sulprizio, M. P., Peng, R. D., Yue, X., Son, J.-Y., Anderson, G. B. and Bell, M. L.: Wildfire-specific Fine Particulate Matter and Risk of Hospital Admissions in Urban and Rural Counties, Epidemiology, 28(1), 77–85, doi:10.1111/mec.13536.Application, 2017.

Liu, Y., Liggio, J. and Staebler, R.: Reactive uptake of ammonia to secondary organic aerosols: Kinetics of organonitrogen formation, Atmos. Chem. Phys., 15(23), 13569–13584, doi:10.5194/acp-15-13569-2015, 2015.

Di Lorenzo, R. A., Place, B. K., VandenBoer, T. C. and Young, C. J.: Composition of Size-Resolved Aged Boreal Fire Aerosols: Brown Carbon, Biomass Burning Tracers, and Reduced Nitrogen, ACS Earth Sp. Chem., 2(3), 278–285, doi:10.1021/acsearthspacechem.7b00137, 2018.

Lowe, A. B.: Thiol-ene “click” reactions and recent applications in polymer and materials synthesis, Polym. Chem., 1(1), 17–36, doi:10.1039/b9py00216b, 2010.

Makar, P. A., Akingunola, A., Aherne, J., Cole, A. S., Aklilu, Y. A., Zhang, J., Wong, I., Hayden, K., Li, S. M., Kirk, J., Scott, K., Moran, M. D., Robichaud, A., Cathcart, H., Baratzedah, P., Pabla, B., Cheung, P., Zheng, Q. and Jeffries, D. S.: Estimates of

711 exceedances of critical loads for acidifying deposition in Alberta and Saskatchewan,
712 Atmos. Chem. Phys., 18(13), 9897–9927, doi:10.5194/acp-18-9897-2018, 2018.
713 Mashkina, A. V.: Catalytic Synthesis Of Sulfides Sulfoxides and Sulfones, Sulfur reports, 10(4),
714 279–388, doi:10.1080/01961779108048759, 1991.
715 McLinden, C. A., Fioletov, V., Krotkov, N. A., Li, C., Boersma, K. F. and Adams, C.: A Decade
716 of Change in NO2 and SO2 over the Canadian Oil Sands As Seen from Space, Environ.
717 Sci. Technol., 50(1), 331–337, doi:10.1021/acs.est.5b04985, 2016.
718 Meng, F. R., Bourque, C. P. A., Belczewski, R. F., Whitney, N. J. and Arp, P. A.: Foliage
719 responses of spruce trees to long-term low-grade sulfur dioxide deposition, Environ.
720 Pollut., 90(2), 143–152, doi:10.1016/0269-7491(94)00101-I, 1995.
721 Murphy, B. N., Donahue, N. M., Robinson, A. L. and Pandis, S. N.: A naming convention for
722 atmospheric organic aerosol, Atmos. Chem. Phys., 14(11), 5825–5839, doi:10.5194/acp-
723 14-5825-2014, 2014.
724 Nozière, B., Kalberer, M., Claeys, M., Allan, J., D'Anna, B., Decesari, S., Finessi, E., Glasius,
725 M., Grgić, I., Hamilton, J. F., Hoffmann, T., Iinuma, Y., Jaoui, M., Kahnt, A., Kampf, C.
726 J., Kourtchev, I., Maenhaut, W., Marsden, N., Saarikoski, S., Schnelle-Kreis, J., Surratt,
727 J. D., Szidat, S., Szmigielski, R. and Wisthaler, A.: The Molecular Identification of
728 Organic Compounds in the Atmosphere: State of the Art and Challenges, Chem. Rev.,
729 115(10), 3919–3983, doi:10.1021/cr5003485, 2015.
730 Nyborg, M., Solberg, E. D., Malhi, S. S., Takyi, S., Yeung, P. and Chaudhry, M.: Deposition of
731 anthropogenic sulphur dioxide on soils and resulting soil acidification, Plant-Soil Interact.
732 Low pH, 147–156, doi:10.1007/978-94-011-3438-5_16, 1991.
733 Onda, Y.: Oxidative protein-folding systems in plant cells, Int. J. Cell Biol., 2013,

734 doi:10.1155/2013/585431, 2013.
735 Pan, Y. P., Wang, Y. S., Tang, G. Q. and Wu, D.: Spatial distribution and temporal variations of
736 atmospheric sulfur deposition in Northern China: Insights into the potential acidification
737 risks, Atmos. Chem. Phys., 13(3), 1675–1688, doi:10.5194/acp-13-1675-2013, 2013.
738 Reid, C. E., Brauer, M., Johnston, F. H., Jerrett, M., Balmes, J. R. and Elliott, C. T.: Critical
739 review of health impacts of wildfire smoke exposure, Environ. Health Perspect., 124(9),
740 1334–1343, doi:10.1289/ehp.1409277, 2016.
741 Rogers, H. M., Ditto, J. C. and Gentner, D. R.: Evidence for impacts on surface-level air quality
742 in the northeastern US from long-distance transport of smoke from North American fires
743 during the Long Island Sound Tropospheric Ozone Study (LISTOS) 2018, Atmos. Chem.
744 Phys., 20(2), 671–682, doi:10.5194/acp-20-671-2020, 2020.
745 Sekimoto, K., Koss, A. R., Gilman, J. B., Selimovic, V., Coggon, M. M., Zarzana, K. J., Yuan,
746 B., Lerner, B. M., Brown, S. S., Warneke, C., Yokelson, R. J., Roberts, J. M. and De
747 Gouw, J.: High-and low-temperature pyrolysis profiles describe volatile organic
748 compound emissions from western US wildfire fuels, Atmos. Chem. Phys., 18(13),
749 9263–9281, doi:10.5194/acp-18-9263-2018, 2018.
750 Sengupta, D., Samburova, V., Bhattarai, C., Kirillova, E., Mazzoleni, L., Iaukea-Lum, M., Watts,
751 A., Moosmüller, H. and Khlystov, A.: Light absorption by polar and non-polar aerosol
752 compounds from laboratory biomass combustion, Atmos. Chem. Phys., 18(15), 10849–
753 10867, doi:10.5194/acp-18-10849-2018, 2018.
754 Sheu, R., Marcotte, A., Khare, P., Charan, S., Ditto, J. C. and Gentner, D. R.: Advances in
755 offline approaches for chemically speciated measurements of trace gas-phase organic
756 compounds via adsorbent tubes in an integrated sampling-to-analysis system, J.

Chromatogr. A, 1575, 80–90, doi:10.1016/j.chroma.2018.09.014, 2018.

Song, J., Li, M., Fan, X., Zou, C., Zhu, M., Jiang, B., Yu, Z., Jia, W., Liao, Y. and Peng, P.: Molecular Characterization of Water- And Methanol-Soluble Organic Compounds Emitted from Residential Coal Combustion Using Ultrahigh-Resolution Electrospray Ionization Fourier Transform Ion Cyclotron Resonance Mass Spectrometry, Environ. Sci. Technol., 53(23), 13607–13617, doi:10.1021/acs.est.9b04331, 2019.

Updyke, K. M., Nguyen, T. B. and Nizkorodov, S. A.: Formation of brown carbon via reactions of ammonia with secondary organic aerosols from biogenic and anthropogenic precursors, Atmos. Environ., 63, 22–31, doi:10.1016/j.atmosenv.2012.09.012, 2012.

Val Martín, M., Honrath, R. E., Owen, R. C., Pfister, G., Fialho, P. and Barata, F.: Significant enhancements of nitrogen oxides, black carbon, and ozone in the North Atlantic lower free troposphere resulting from North American boreal wildfires, J. Geophys. Res. Atmos., 111(23), 1–17, doi:10.1029/2006JD007530, 2006.

Vicente, A., Alves, C., Calvo, A. I., Fernandes, A. P., Nunes, T., Monteiro, C., Almeida, S. M. and Pio, C.: Emission factors and detailed chemical composition of smoke particles from the 2010 wildfire season, Atmos. Environ., doi:10.1016/j.atmosenv.2013.01.062, 2013.

Wang, X., Wang, H., Jing, H., Wang, W. N., Cui, W., Williams, B. J. and Biswas, P.: Formation of Nitrogen-Containing Organic Aerosol during Combustion of High-Sulfur-Content Coal, Energy and Fuels, 31(12), 14161–14168, doi:10.1021/acs.energyfuels.7b02273, 2017a.

Wang, X. K., Rossignol, S., Ma, Y., Yao, L., Wang, M. Y., Chen, J. M., George, C. and Wang, L.: Molecular characterization of atmospheric particulate organosulfates in three megacities at the middle and lower reaches of the Yangtze River, Atmos. Chem. Phys.,

16(4), 2285–2298, doi:10.5194/acp-16-2285-2016, 2016.

Wang, X. K., Hayeck, N., Brüggemann, M., Yao, L., Chen, H., Zhang, C., Emmelin, C., Chen, J., George, C. and Wang, L.: Chemical Characteristics of Organic Aerosols in Shanghai: A Study by Ultrahigh-Performance Liquid Chromatography Coupled With Orbitrap Mass Spectrometry, J. Geophys. Res. Atmos., 122(21), 11,703-11,722, doi:10.1002/2017JD026930, 2017b.

Ward, D. E.: Factors Influencing the Emissions of Gases and Particulate Matter from Biomass Burning, in Fire in the Tropical Biota: Ecosystem Processes and Global Challenges, pp. 418–436., 1990.

Wong, J. P. S., Tsagkaraki, M., Tsiodra, I., Mihalopoulos, N., Violaki, K., Kanakidou, M., Sciare, J., Nenes, A. and Weber, R. J.: Effects of Atmospheric Processing on the Oxidative Potential of Biomass Burning Organic Aerosols, Environ. Sci. Technol., 53(12), 6747–6756, doi:10.1021/acs.est.9b01034, 2019.

Yokelson, R. J., Burling, I. R., Gilman, J. B., Warneke, C., Stockwell, C. E., De Gouw, J., Akagi, S. K., Urbanski, S. P., Veres, P., Roberts, J. M., Kuster, W. C., Reardon, J., Griffith, D. W. T., Johnson, T. J., Hosseini, S., Miller, J. W., Cocker, D. R., Jung, H. and Weise, D. R.: Coupling field and laboratory measurements to estimate the emission factors of identified and unidentified trace gases for prescribed fires, Atmos. Chem. Phys., 13(1), 89–116, doi:10.5194/acp-13-89-2013, 2013.

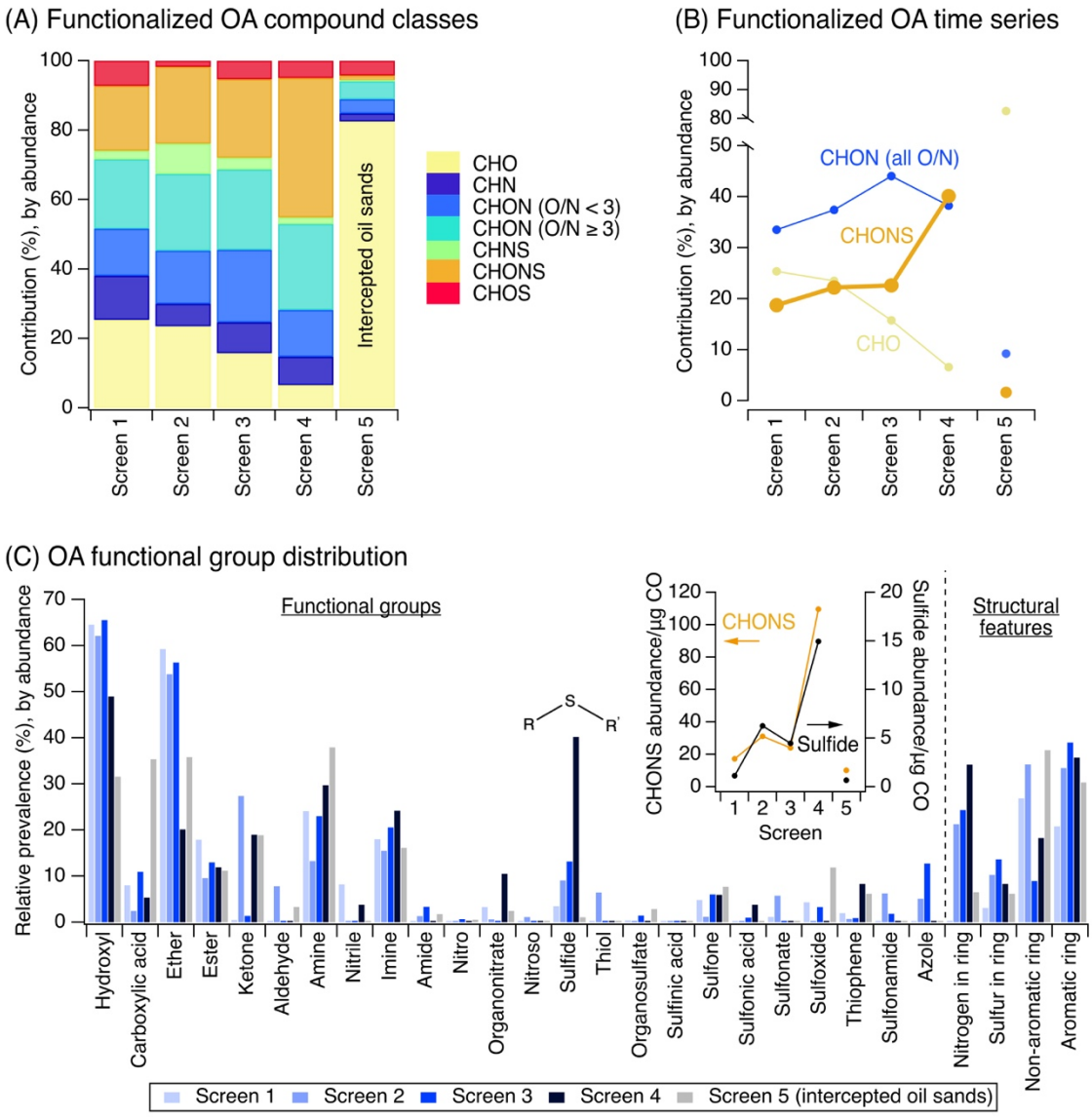

Figure 1. (A) The compound class distribution of functionalized OA (from non-targeted LC-ESI-MS) weighted by ion abundance, shown as percent contribution of each compound class to the total compound abundance measured by LC-ESI-MS. (B) Percent contribution of CHO, CHON, and CHONS compound classes in functionalized OA as a function of plume age. CHON compounds in panel B are summed across all O/N ratios. (C) Functional groups and structural features present in measured functionalized OA (from non-targeted LC-ESI-MS/MS). The sulfide functional group is shown here for emphasis, and will be the subject of subsequent analyses. The inset in panel C shows the absolute CHONS ion abundance normalized by CO mass (orange trace, left y-axis) and the absolute sulfide ion abundance normalized by CO mass (black trace, right y-axis). Full CO-adjusted compound class and functional group abundance data are shown in Figures S5-S6. For panels A-C, results tabulated by occurrence are also shown in Figure S5-S6.

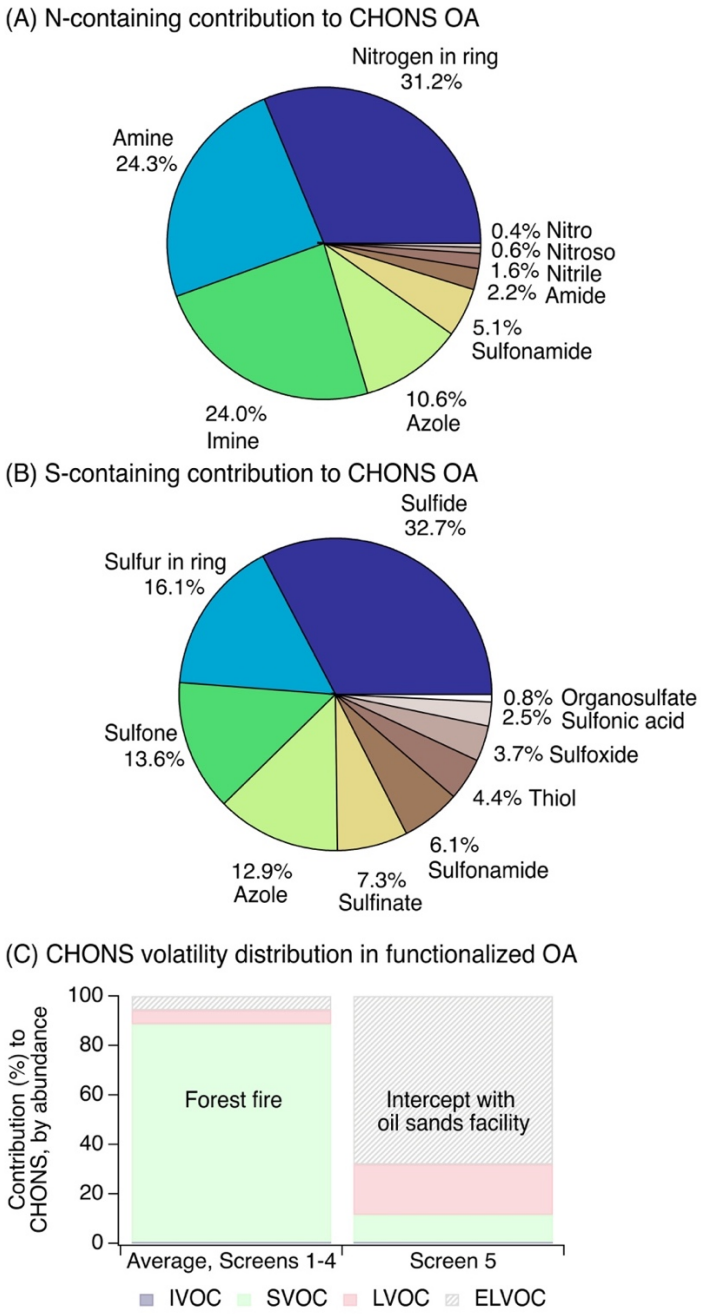

811 **Figure 2.** (A) The distribution of nitrogen-containing functional groups to particle-phase
812 CHONS compounds (organonitrates are excluded here due to challenges with their identification
813 using SIRIUS with CSI:FingerID, but contributed minimally to CHONS, Supporting Information
814 S3). (B) The distribution of sulfur-containing groups to particle-phase CHONS compounds.
815 For panels A-B, data are averaged across screens 1-4, with individual screens shown in Figure
816 S7A. (C) Volatility distribution of particle-phase CHONS species. These volatility data were
817 averaged across screens 1-4, and individual screens are shown in Figure S8. Volatility was
818 estimated with the parameterization in Li et al. (Li et al., 2016) and grouped according to
819 volatility bins in Donahue et al. (Donahue et al., 2011).

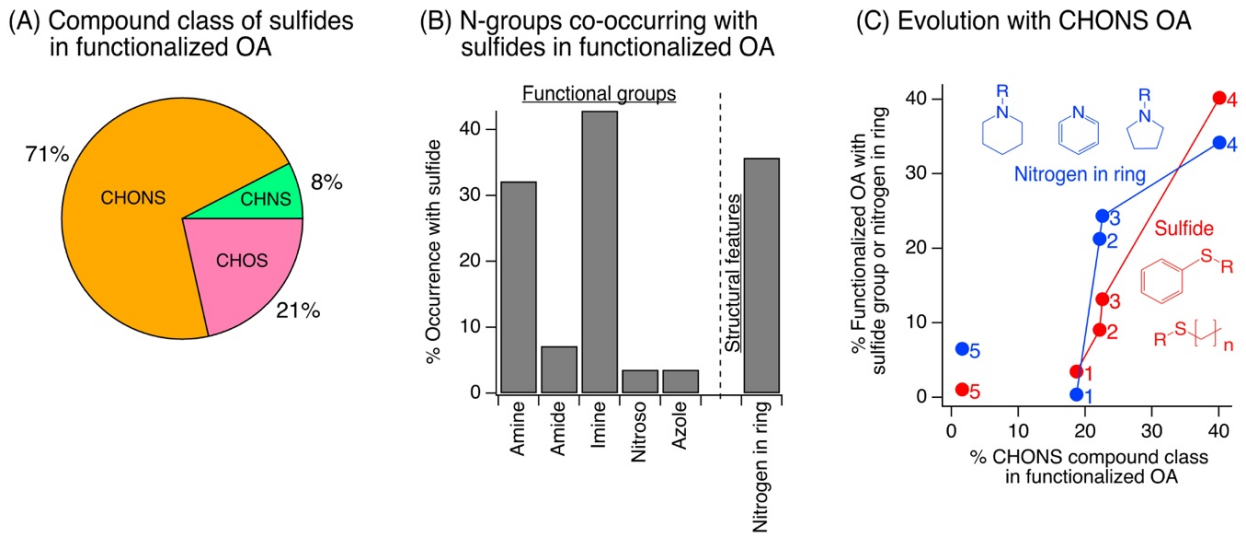

820 **Figure 3.** (A) Compound class distribution of sulfide groups: 71% of sulfide functional groups
821 observed (weighted by ion abundance) were present in CHONS compounds. (B) Co-occurrence
822 of sulfides and nitrogen-containing groups. Data shown in panels A-B are cumulative across
823 compounds in screens 1-4. (C) The relative contribution of sulfides and cyclic nitrogen groups to
824 all functionalized OA increased together with the increasing contribution of CHONS
825 compounds. The other functional groups in panel B showed no relationship with the increase in
826 CHONS (Figure S7B). Structures represent examples of commonly observed sulfide and cyclic
827 nitrogen substructures from SIRIUS and CSI:FingerID (Supporting Information S3), where ring
828 structures associated with nitrogen heteroatoms were free standing, adjacent to other rings,
829 and/or contained additional attached functional groups.

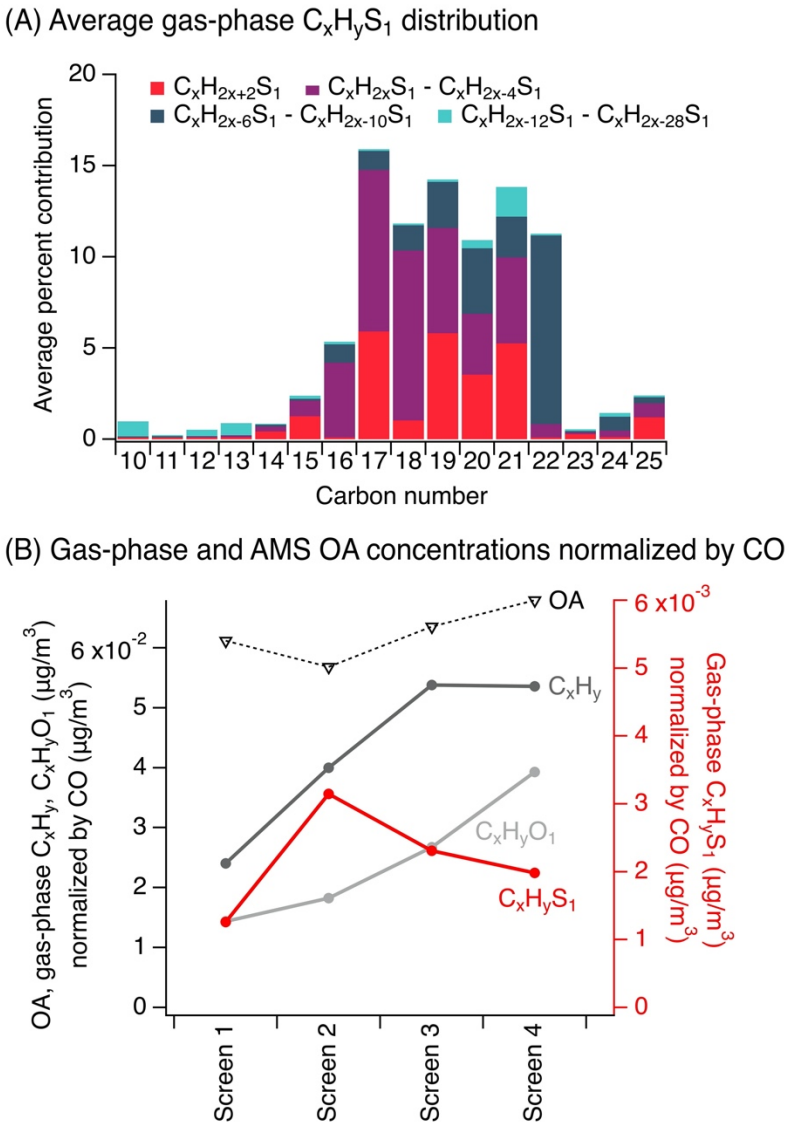

Figure 4. (A) The average $C_xH_yS_1$ distribution from targeted GC-APCI-MS across all gas-phase adsorbent tube samples from screens 1-4 (see Figure S10 for individual $C_xH_yS_1$ screens, and Figure S13 for C_xH_y). (B) Concentrations of gas-phase C_xH_y, $C_xH_yO_1$, $C_xH_yS_1$ from targeted GC-APCI-MS analysis of adsorbent tubes, shown with total OA from AMS, all corrected for dilution using carbon monoxide measurements (see Figure S12A for non-normalized concentrations). Data in panel B are averaged over low and high altitude adsorbent tube samples.

Supporting Information:

Atmospheric Evolution of Emissions from a Boreal Forest Fire: The Formation of Highly-Functionalized Oxygen-, Nitrogen-, and Sulfur-Containing Organic Compounds

Jenna C. Ditto[1], Megan He[1], Tori N. Hass-Mitchell[1], Samar G. Moussa[2], Katherine Hayden[2], Shao-Meng Li[2], John Liggio[2], Amy Leithead[2], Patrick Lee[2], Michael J. Wheeler[2], Jeremy J.B. Wentzell[2], Drew R. Gentner[1,3,*]

[1] Department of Chemical and Environmental Engineering, Yale University, New Haven, CT, 06511, USA; [2] Air Quality Research Division, Environment and Climate Change Canada, Toronto, Ontario M3H 5T4, Canada; [3] Solutions for Energy, Air, Climate and Health (SEARCH), School of the Environment, Yale University, New Haven CT 0651, USA

* Correspondence to: drew.gentner@yale.edu

S1. Supporting sample collection details

The gas- and particle-phase samples discussed here were collected alongside a variety of other measurements including trace gas mixing ratios (e.g. NO_x, O_3, CO, CO_2, CH_4, NH_3), black carbon concentrations, and gas- and particle-phase chemical characterization via online mass spectrometry. Carbon monoxide mixing ratios, select gas-phase tracer mixing ratios from PTR-ToF-MS, and AMS organic aerosol (OA) concentrations were used as supporting data in this study.

Carbon monoxide mixing ratios were measured with a Picarro G2401 analyzer every 2 seconds during the flights. When absolute ion abundances from adsorbent tube or filter data were used to discuss in-plume chemical transformations, abundances were normalized by the total carbon monoxide mass observed during the corresponding sampling period.

A proton transfer reaction time-of-flight mass spectrometer (PTR-ToF-MS, Ionicon Analytik GmbH, Austria) was installed on the aircraft and collected measurements of volatile organic compounds (VOCs) with a time resolution of 1 second during the flights. The PTR-ToF-MS used a proton transfer reaction with H_3O^+ as the primary reagent ion. VOCs were separated according to their mass to charge (*m/z*) ratio and detected using a high resolution time-of-flight mass spectrometer. The data were processed using the TOFWARE software (Tofwerk AG). Additional details on these methods can be found in past work (Li et al., 2017).

A high resolution aerosol mass spectrometer (AMS, Aerodyne Inc) was used to measure mass concentrations of aerosol-phase organics, NO_3, SO_4 and NH_4 (only organics are discussed here). Using an aerodynamic lens, particles were sampled into a region of low vacuum where they impacted a heated surface (600°C), were vaporized, and then ionized by 70 eV impaction. Ions were detected with a time-of-flight mass spectrometer. The AMS was operated in V mode

with 10 second time resolution. A collection efficiency of 0.5 was determined using the method from Middlebrook et al. (Middlebrook et al., 2012), and applied to the data. The collection efficiency was also estimated by comparing the total mass concentrations with those derived from the UHSAS onboard the aircraft (ultra-high sensitivity aerosol spectrometer). UHSAS volume concentrations were converted to mass concentrations using densities weighted by the AMS components. Both methods yielded similar results.

S1.1. Adsorbent tubes: Combined gas- and particle-phase samples were collected on adsorbent tubes using a novel wing pod sampler (Figure S2) and integrated across a set of low and high altitudes in screens 1-4 (Figure S1, Table S1). The wing pod (a standard PMS canister) contained multiple adsorbent tubes, selection valves, a flow meter, a pump, and control and data acquisition electronics. The wing pod sample inlet consisted of a 7" long Teflon tube (1/8" diameter), connected to an inlet manifold for distribution to multiple installed adsorbent tubes (Figure S2). The small length of Teflon inlet tubing and manifold were designed as the only upstream components to have potential contact with the air sample before it entered the adsorbent tubes (residence time ~0.3 seconds). The inlet manifold was heated to slightly above ambient temperature, with temperature monitored by the control software. Solenoid valves were positioned downstream from each adsorbent tube to remotely switch the air flow through any one single tube at a time. Air was drawn through the selected tube by a small DC pump with an orifice and mass flow meter (Alicat Scientific) regulating and monitoring flow. A temperature/pressure sensor was attached on the inlet manifold for monitoring the thermophysical properties of sampled air. All flows, valve positions, temperatures, and pressures were recorded using a data acquisition board (LabJack T7) integrated into the pod.

Communications with the pod were performed via the aircraft's internal Ethernet network using custom LabVIEW software. This remote access allowed sampling to be triggered by an operator in flight, while minimizing the amount of sample inlet needed to supply ambient air to the adsorbent tubes.

The total adsorbent tube sampling times ranged from 4-52 minutes (depending on the time required to complete a set of transects) at an average flow rate of 285 sccm, yielding a total sample volume of ~1-15 L. These sampling times and flow rates were similar to those tested extensively in past work with the same adsorbent tubes (e.g. 6-25 L at 125-250 sccm (Sheu et al., 2018)), though the slightly higher flow rate in our study was verified to confirm minimal analyte breakthrough. VOCs from a mixture of C_6-C_{13} species were used (hydrocarbons and functionalized species from a multicomponent gas cylinder mixture (Apel-Riemer)), consistent with past breakthrough testing with the same adsorbent tubes (Sheu et al., 2018). Our results showed good retention when adsorbent tubes were tested at 300 sccm for 15 up to 60 minutes (7% loss on average), with some loss of C_6-C_9 compounds at longer sampling times (13% loss on average). Therefore, this study was focused on hydrocarbons and functionalized species C_{10} and larger, to ensure that compounds had similar or lower volatility than the breakthrough test analyte sets, and thus similar or greater retention in the adsorbent tubes during field sampling.

To correct for any background contamination in subsequent data analyses, field blank adsorbent tubes were collected throughout the campaign by installing adsorbent tubes in the wing pod sampler during flight without sampling on them. All adsorbent tubes were spiked with a deuterated standard (containing n-hexadecane-d34, diethyl phthalate-d4, benz(a)anthracene-d12, n-octane-d18, ethylbenzene-d10, octanoic acid-d15, benzene-d6, and n-dodecanol-d25), and stored with 1/4" brass Swagelok caps in a -30°C freezer before analysis.

S1.2. Filters: Particles were sampled through a forward-facing isokinetic diffuser inlet (DMT) mounted on the roof of the aircraft. Particles with diameters approximately <2.5 μm were expected to be transmitted through this sampling setup based on transmission efficiency calculations using inlet dimensions and volume flow rates. Particles were collected onto PTFE filters using a multi-filter holder assembly mounted in the cabin of the aircraft. Filter sampling times ranged from 29-101 minutes, at an average flow rate of 46 L/min. One filter sample was collected per screen for screens 1-5 (Figure S1, Table S1).

Similar to adsorbent tube methods, filter field blanks were collected throughout the campaign by installing filters in the sampler with no air flow. Filters were spiked with the same deuterated standard discussed above, and stored in closed sterile petri dishes in a -30°C freezer before analysis.

S2. Supporting analytical methods details

S2.1. Adsorbent tubes: Adsorbent tubes were run on a GERSTEL Thermal Desorber TD 3.5+, with a 6 minute dry purge at 100 mL/min helium flow at 35°C to eliminate excess water trapped on the tubes, followed by a 10 minute desorption at 310°C, trapping desorbed analytes in the GERSTEL Cooled Injection System (CIS) at -100°C. Tubes were spiked with a range of standards (the multicomponent gas cylinder mixture discussed above, in addition to a set of functionalized liquid standards with a range of oxygen-, nitrogen-, and sulfur-containing functional groups from Sigma Aldrich and AccuStandard (Ditto et al., 2018, 2020)) to evaluate possible losses associated with dry purging. While some losses of higher volatility compounds were observed as expected (Ochiai et al., 2014), analytes generally showed good retention (~86% retained on average) during this preparatory step (Figure S4). CIS contents were

subsequently desorbed at 325°C onto a DB5-MS-UI GC column (30 m x 320 μm x 0.25 μm). The column was held at 35°C for 5 minutes, followed by a 10°C/minute ramp to 325°C, and a 3-minute hold at 325°C. Helium carrier gas flowed through the column at 1.5 mL/min. The APCI source was operated in positive mode and the Q-TOF was operated in MS mode, following methods in past work (Khare et al., 2019).

Daily system check standards were run with adsorbent tube samples, including diluted diesel fuel (#2 diesel fuel from AccuStandard, DRO-AK-102-LCS-10X-R1) to confirm calibration and transmission of a complex hydrocarbon mixture through the analytical system, along with a mixture of hydrocarbons and functionalized species from the multicomponent gas cylinder mixture discussed above (Sheu et al., 2018). NIST Reference Gulf of Mexico 2779 Macondo Crude Oil was also run for response factor mass calibrations across the analyte range of interest, discussed in Section S3 (Khare et al., 2019).

S2.2 Filters: Filters were extracted in methanol with 60 minutes of sonication, and solvent was evaporated down to 200 μL under gentle N_2 flow (Ditto et al., 2018). Next, 5 μL aliquots were analyzed on an SBAQ reverse phase column using water (A) and methanol (B) as mobile phases, running the following solvent gradient: 95% (A) for 2 minutes, then solvents ramped to 10% A and 90% B for 20 minutes, then held at 10% A and 90% B for 5 minutes, and finally returned to initial conditions for the next run (Ditto et al., 2018). The ESI source was operated in positive and negative ionization mode, and the Q-TOF was operated in both MS and MS/MS mode, following previously described methods (Ditto et al., 2018, 2020). All data discussed here report both positive and negative mode peaks; when a compound ionized well in both modes, its abundances in positive and negative mode were averaged, and it was only tabulated once.

Filter extracts were also analyzed via GC-APCI-MS using the GERSTEL TD 3.5+. For GC-APCI-MS analysis, 1 μL aliquots were automatically injected by the GERSTEL system into the TD inlet. The inlet was subsequently desorbed at 310°C for 10 minutes, while trapping analytes on the CIS at -100°C, as described above. The APCI and Q-TOF operating conditions were the same as for adsorbent tubes.

Daily system checks using authentic standards were run with filter samples on LC and GC, focusing on a set of functionalized liquid standards with a range of oxygen-, nitrogen-, and sulfur-containing functional groups (discussed above). These standards were used to determine an average response factor of functionalized analytes, which was in turn used to estimate mass concentration analyzed with the filter samples (Section S4).

In addition, as part of data quality control for both adsorbent tubes and filters, we performed a targeted search through sample data for common biomass burning tracers such as levoglucosan, benzenediols, methoxyphenols, vanillin, vanillic acid, acetovanillone, and dehydroabietic acid, among others. However, the goal of this study was to examine the complex mixture in forest fire smoke and to study molecular-level trends in the evolution of the mixture as a whole. As such, the methods applied here for sample analysis and data analysis were geared towards this purpose, rather than to focus on particular tracer compounds, which were targeted by other instruments in the aircraft payload (e.g. PTR-ToF-MS). While several of these tracers were outside of the carbon number range of interest in this study, we searched for them in the adsorbent tube and filter data to ensure that our methods captured a range of expected biomass burning emissions and transformation products based on past field and laboratory observations (e.g. levoglucosan was observed in the particle phase across all 5 screens; vanillin and

acetovanillone were observed in all 4 screens of gas-phase measurements; vanillic acid was observed prominently in both phases (Schauer et al., 2001; Simoneit et al., 1993)).

S3. Supporting data analysis methods details

There are two types of analyses discussed in this work: non-targeted (primarily for particle-phase LC-ESI-MS, LC-ESI-MS/MS, and GC-APCI-MS) and targeted (primarily for gas-phase GC-APCI-MS). The details of both approaches are discussed in previous work, but we summarize the important points here.

S3.1 Non-targeted analysis and QA/QC for particle-phase samples: In brief, for non-targeted analysis, the Q-TOF examined mass spectra across the entire LC elution time for a particular sample. Peak, formula, and structural identifications were extensively quality controlled (including subtraction of any contaminants or artifacts from field blanks, and elimination of low quality peaks and formula/structural identifications (Ditto et al., 2018, 2020)) but were not restricted to target a particular set of compounds. Elemental formula parameters were set to $C_{3–60}H_{4–122}O_{0–20}N_{0–3}S_{0–1}$, and no significant change in top-ranked identifications was observed when expanding the nitrogen and sulfur elemental counts. For LC-ESI-MS/MS analysis, mass spectra were imported to SIRIUS with CSI:FingerID, and this software was used to predict structures. We note that in this study, we did not focus on exact molecular configurations but rather the presence or absence of functional groups, similar to past work (Ditto et al., 2020). We also note that organonitrates were tallied according to prior approaches; this functional group was poorly identified by SIRIUS and CSI:FingerID, so characteristic neutral losses were used to identify organonitrates (see reference for further discussion (Ditto et al., 2020)). However, as a result, the

co-occurring functional groups on organonitrate compounds (predicted by SIRIUS and CSI:FingerID) were assumed to be invalid. So, organonitrates were included in the functional group tally shown in Figure 1C and Figure S6, but not in any subsequent analyses of functional group co-occurrence. The effect of this exclusion was minor since organonitrates had minimal presence in the particle phase in this relatively fresh forest fire plume (~3% on average; Figure 1C). In addition, nitrogen or sulfur atoms in non-aromatic rings were tallied both as a "nitrogen in ring" or "sulfur in ring" (Figure 1C) *and* as any other applicable functional group (e.g. amine, sulfone). Hence, they are reported separately as structural features throughout the manuscript (e.g. Figure 1C, Figure S6-S7A). Importantly, we note that none of the sulfide-containing compounds identified in this work were present as ring-bound sulfur.

S3.2. Targeted analysis and QA/QC for gas-phase samples: For targeted analysis, we searched for specific large sets of molecular ions across C_{10}-C_{25} with double bond equivalents (DBE) or corresponding degrees of unsaturation from 0-15 for C_xH_y, $C_xH_yO_1$, $C_xH_yS_1$, and $C_xH_yN_1$ compound classes. While some compounds with a greater heteroatom count could be present in the adsorbent tube (i.e. gas-phase) samples, heteroatom counts were limited to one for each compound class to facilitate the targeted ion search. We focused on this carbon number range to supplement other on-board instrumentation measuring VOCs (i.e. PTR-ToF-MS) and also because the adsorbent tubes' sampling and analytical conditions were optimized for this range of molecular weights.

Peaks for each ion were extracted at 10 ppm mass tolerance and integrated with custom Igor Pro code. Samples were all blank subtracted (using field blanks), and known contaminants and artifacts were removed. Peak areas for C_xH_y ions were converted to mass using a C_xH_y

response factor for individual carbon numbers and DBEs, determined based on the known distribution of carbon numbers and DBEs in the NIST Gulf of Mexico 2779 Macondo Crude Oil standard with GC and soft ionization (Khare et al., 2019; Worton et al., 2015). To convert $C_xH_yO_1$ and $C_xH_yS_1$ peak areas to mass, we applied the average C_xH_y response factors for aromatic compounds (which had limited fragmentation in the APCI source) based on an intercomparison of mass responses from available oxygen- and sulfur-containing individual authentic standards, evaluations of fragmentation patterns of these functionalized species, and determination of an analogous carbon number based on the volatility difference introduced by adding an oxygen or sulfur heteroatom to a C_xH_y hydrocarbon, as discussed in past work (Khare et al., 2020). This resulted in shifting the average response factors up by 1 or 2 carbon numbers when accounting for the presence of oxygen or sulfur heteroatoms, respectively, and accounting for the ratio of $[M+H]^+$ to $[M]^+$ ion abundance observed. $C_xH_yO_1$ and $C_xH_yS_1$ response factors were based on the C_xH_y response factor because of limited availability of individual oxygen- or sulfur-containing standards across the entire carbon number and structural range, and because of greater structural ambiguity in these complex functionalized mixtures (due to a range of possible oxygen- and sulfur-containing functional groups and the possibility of double bonds both in the carbon backbone structure and in the functional group itself). We acknowledge that this approach comes with added uncertainty and apply it here to provide useful context for the relative mass of $C_xH_yO_1$ and $C_xH_yS_1$ compared to C_xH_y. However, it is critical to note that the uncertainty in the conversion from peak area to mass does not affect our results that describe trends across screens and the diversity of molecular size and structure observed (e.g. straight/branched vs. aromatic)—these features were all observed in the ion abundance data prior to mass estimation. $C_xH_yN_1$ was studied here in terms of peak area only.

The vast majority of the total compound mass observed via targeted analysis of adsorbent tube samples in the C_{10}-C_{25} range should have existed in the gas phase. This is based in part on significant undersampling for particles at the adsorbent tube inlet (discussed in the main text). This is also based on partitioning coefficients calculated with estimated aerosol loading (from AMS OA concentration data, Figure 4B) and the approximate saturation mass concentration for this carbon number range (Equation 1, from Donahue et al., 2009) (Donahue et al., 2009, 2011):

$$\xi_i = \frac{1}{1+\frac{C_i^*}{C_{OA}}} \quad [1]$$

In Equation 1, ξ_i is a partitioning coefficient of compound i, C_i^* is the effective saturation concentration of compound i, and C_{OA} is the mass concentration of the existing organic particle phase. As shown in Table S2, compounds below ~C_{22}-C_{23} should have existed mostly in the gas phase, though compounds ~C_{20} and up would have readily partitioned from and equilibrated with the particle phase with small changes in OA concentration. This range of observed compounds therefore had likely contributions from semivolatile particle-phase species evaporating with plume dilution, as discussed in the main text in Section 3.3 and Figure 4B.

S4. Representativeness of mass analyzed via filter and adsorbent tube samples

The analysis of particle-phase samples discussed here used methods geared towards functionalized OA, i.e. OA with one or more oxygen-, nitrogen-, and/or sulfur-containing functional groups or structural features. Samples were extracted in methanol due to its effectiveness at extracting polar analytes from similar filter media in past studies (Ditto et al., 2018; Ng et al., 2008; Riva et al., 2016a, 2016b; Seinfeld et al., 2008); no distinct trends were observed that suggested major differences in extraction efficiency among heteroatom-containing compounds.

Samples were analyzed using electrospray ionization (ESI), which is sensitive towards compounds with oxygen-, nitrogen-, and/or sulfur-containing functional groups that readily interact with protons and other ions in the mobile phase solvents to form charged adducts. For particle-phase samples analyzed with LC-ESI-MS, CH and CHS compound classes were not measured, as they ionized poorly in the ESI source (Ditto et al., 2018, 2019). For these same particle-phase samples analyzed via GC-APCI-MS, CH and CHS were measured (due to improved ionization via APCI), but the contribution of CH was likely underestimated due to fragmentation of alkanes in the ionization source (discussed in Figure S5 and explicitly calibrated for in the targeted adsorbent tube analysis focused on gas-phase compounds (Khare et al., 2019)) and due to possible CH/CHS solubility limitations in the methanol extraction solvent.

Though not designed to be an exact intercomparison for mass closure, we evaluated the total mass analyzed from the filters (via LC-ESI, since these results are the ones primarily displayed and discussed throughout the manuscript) and adsorbent tubes (via GC-APCI) in this study. The sample preparation and analysis methods for filters were tailored for the analysis of functionalized OA; an estimate of functionalized compound mass loading from non-targeted LC-ESI-MS analysis of filter samples with average ESI response factors (Ditto et al., 2018) suggested that these functionalized components represented an average of 26 ± 6 $\mu g/m^3$ across screens 1-4. For comparison, the average AMS OA mass concentration across these same filter sampling times was 31± 5 $\mu g/m^3$. However, there is evidence in this and in past studies for an important contribution from non-functionalized biomass burning OA (i.e. CH compounds) (Corrigan et al., 2013; Zhou et al., 2017), which would not be measured by the filter sampling methods discussed here. This suggests that these LC-ESI and AMS methods may have measured some overlapping but some differing subsets of OA mass. For comparison, adsorbent tube

samples contained 21 ± 6 μg/m^3 of gas-phase C_xH_y, $C_xH_yO_1$, and $C_xH_yS_1$ compounds, from targeted search results in the C_{10}-C_{25} range.

In LC-ESI-MS, we have observed response factors for individual standards to vary across complex mixtures with evident but uncertain relationships to compound classes and functional groups, resulting in sensitivity differences between compounds in the ESI source. In this and in past work, we compared compounds across these diverse multi-functional mixtures by both occurrence and abundance. For the latter, it was necessary to assume an equal ionization efficiency across all compounds (and thus an identical average response factor) because of the challenges associated with assigning compound-specific ionization efficiencies to hundreds of multifunctional compounds in a complex mixture without sufficient reference standards (Ditto et al., 2020). Thus, for comparison, we showed results tabulated both by occurrence and by abundance where applicable (e.g. Figure S5, S6, S8, S9). Results tabulated by occurrence were otherwise not used in any of the analyses discussed here, and were provided as supporting data to aid in the interpretation of results.

S5. Differences in LC and GC results for particle-phase data

As mentioned in *Materials and Methods,* we observed compounds with different oxygen, nitrogen, and sulfur content in LC-ESI and GC-APCI measurements for particle-phase filter samples, resulting from differences in chromatographic and ionization approaches. LC is better suited for more polar compounds that are less volatile and contain more functional groups. In contrast, GC-amenable compounds tend to be less polar and more thermally stable, with overall less functionality. ESI is very sensitive towards functionalized species (e.g. that can be readily protonated or deprotonated), while APCI in the configuration used here can more effectively

ionize less polar analytes (Kondyli and Schrader, 2019). For example, particle-phase compounds from filter samples observed via non-targeted LC-ESI analysis contained an overall average of 4.7 oxygen atoms, with $\overline{O/C}$ = 0.4. Nitrogen-containing compounds had an $\overline{O/N}$ = 2.5, and sulfur-containing compounds had an $\overline{O/S}$ = 5.0. In contrast, compounds from these same filter samples observed via non-targeted GC-APCI analysis contained an overall average of 2.1 oxygen atoms, with $\overline{O/C}$ = 0.2. Nitrogen-containing compounds had an $\overline{O/N}$ = 1.8, and sulfur-containing compounds had an $\overline{O/S}$ = 3.3. An estimate of carbon oxidation state for CH and CHO compounds (Kroll et al., 2011) yielded $\overline{OSc}$ = -0.5 for LC-ESI filter samples and a less oxidized $\overline{OSc}$ = -1.3 for GC-APCI filter samples.

An analysis of filter extracts with non-targeted GC-APCI-MS (Figure S5) showed greater contributions of carbon-, hydrogen-, and oxygen-containing (CHO) and carbon- and hydrogen-containing (CH) compound classes than non-targeted LC-ESI-MS because these compound classes are more GC-amenable, while LC-ESI-MS highlighted contributions from more functionalized species, along with CHO species. As the complex mixture of compounds in the forest fire plume aged, it became increasingly functionalized and likely less GC-amenable. Thus, using exclusively GC techniques to study the evolution of smoke plumes may miss more functionalized, non-GC amenable compounds. Here, we focused on LC-ESI-MS data for the particle phase to study these functionalized species. While LC-ESI-MS does not ionize CH and CHS compound classes effectively, these were outside the scope of our study.

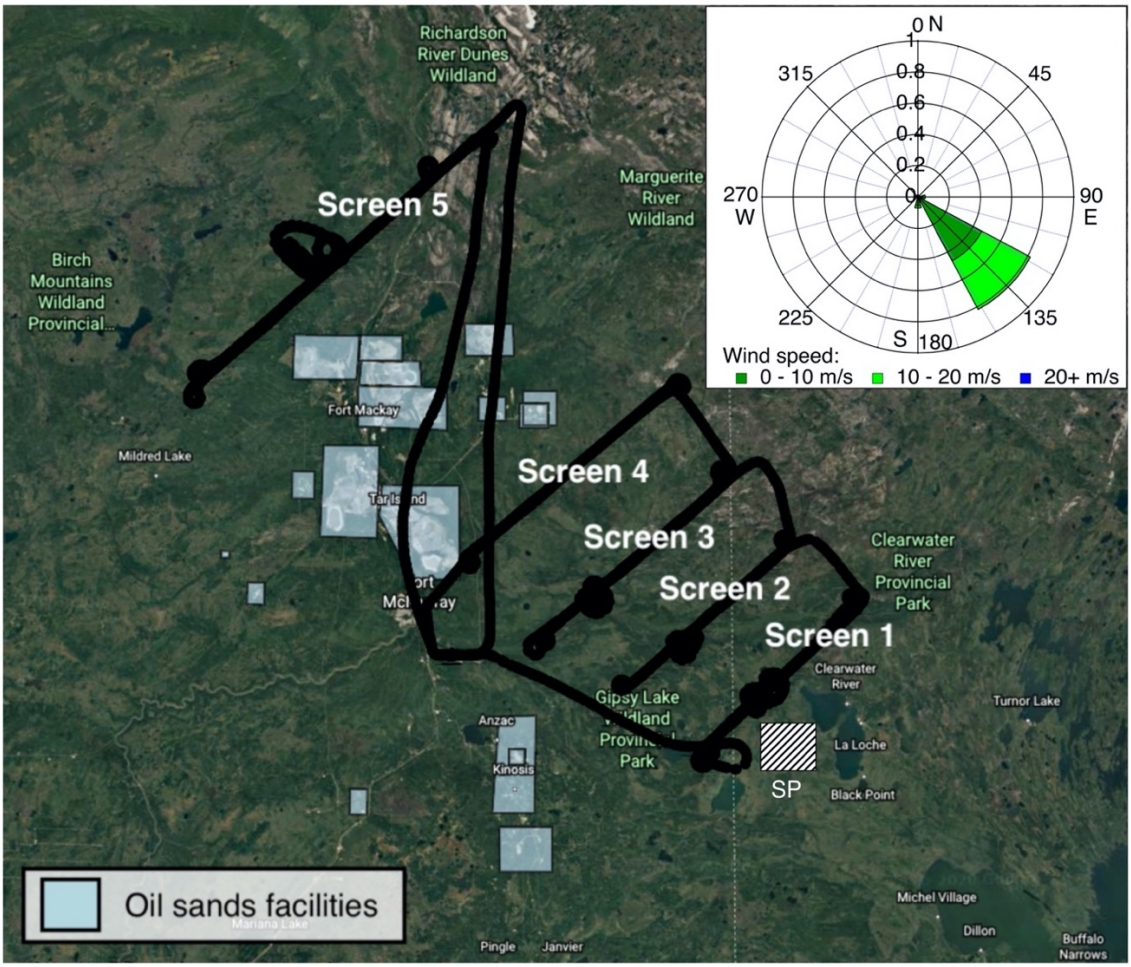

Figure S1. The flight path tracking the forest fire plume on June 25, 2018. Shaded blue regions represent local oil sands processing facilities. Cross hatching represents approximate location of the fire source, located ~10 km from screen 1 (SP is the south plume, whose source was identified via satellite imagery; the north plume source was not identified via satellite imagery, so it is not explicitly shown here but was ~8-19 km to the northeast of the SP at screen 1 and both plumes were estimated to be approximately the same age). Screens 1 and 2 were ~26 km apart, screens 2 and 3 were ~24 km apart, screens 3 and 4 were ~29 km apart, and screens 4 and 5 were ~83 km apart. Prevailing winds were from the southeast during the sampling period as shown by the wind rose in the upper right. Map used to plot flight tracks: © Google Earth: Google, Maxar Technologies.

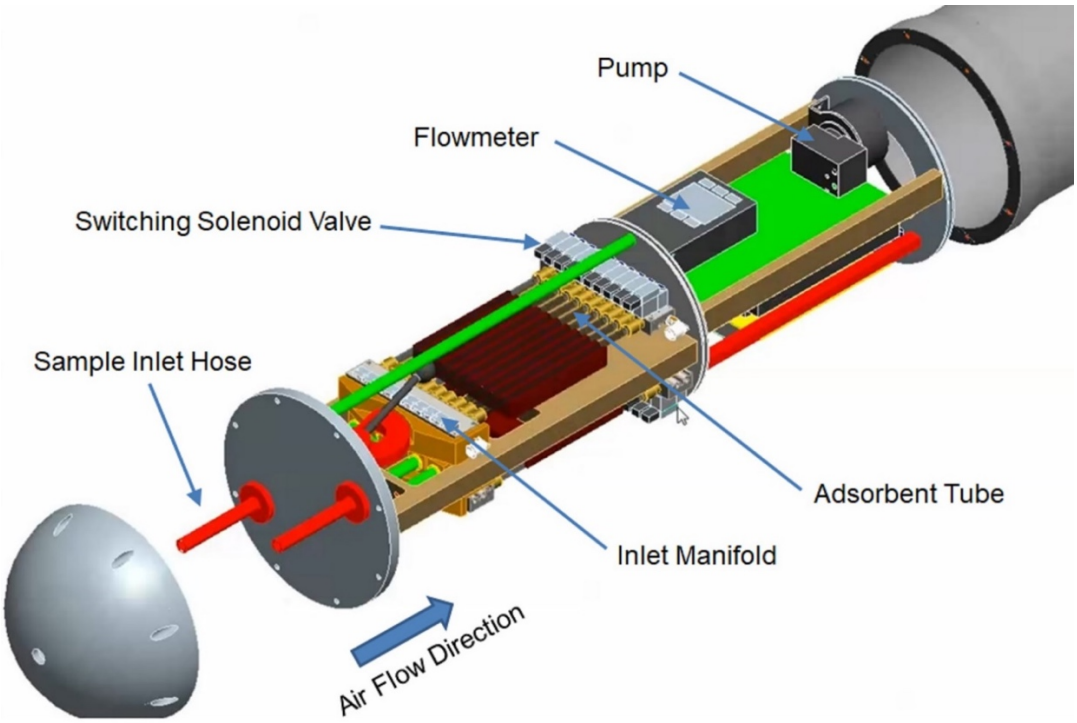

Figure S2. Drawing depicting the key components of the wing pod sampler. Teflon tubing (7" long, 1/8" diameter) was connected to the sample inlet hose and to the inlet manifold. A temperature and pressure sensor was attached to the inlet manifold to monitor the properties of sampled air. Adsorbent tubes for the entire flight were loaded into the sampler, and each tube was connected to the manifold. A solenoid valve was positioned downstream of each adsorbent tube to remotely switch air flow between samples. A flow meter and pump were installed further downstream to control air flow.

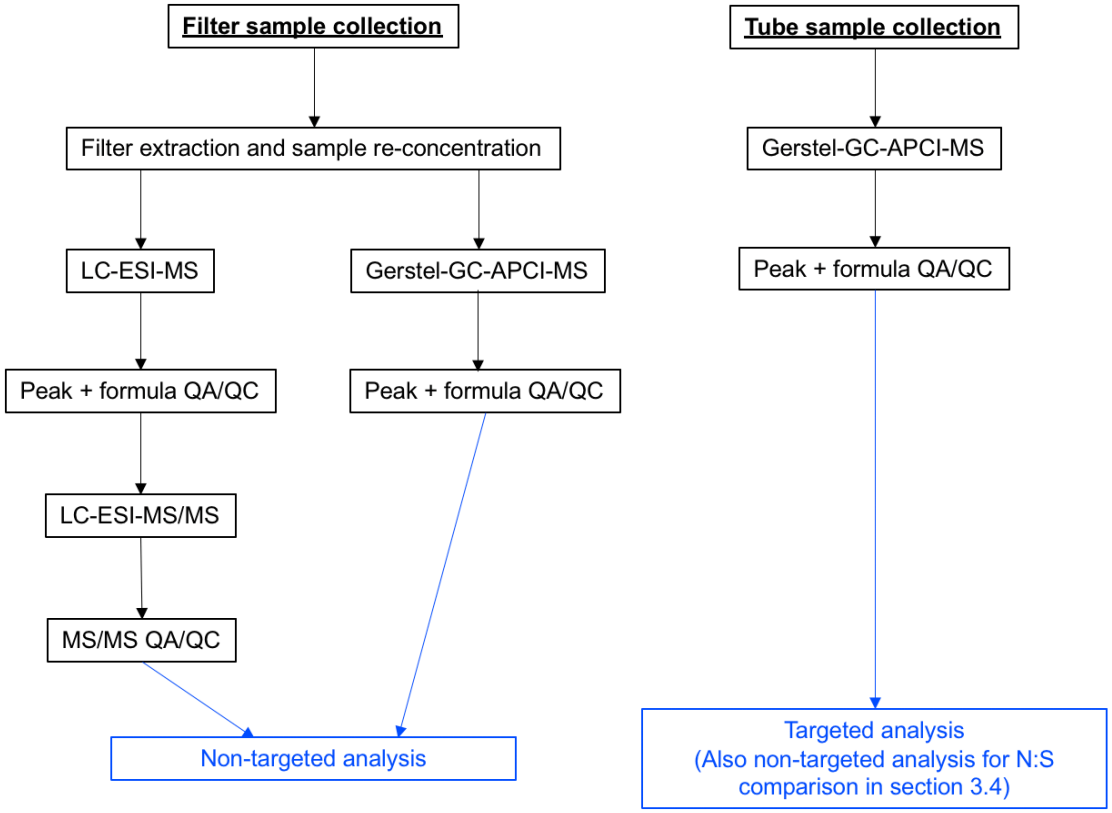

335 **Figure S3.** Summary of adsorbent tube and filter sample collection methods and data analysis.

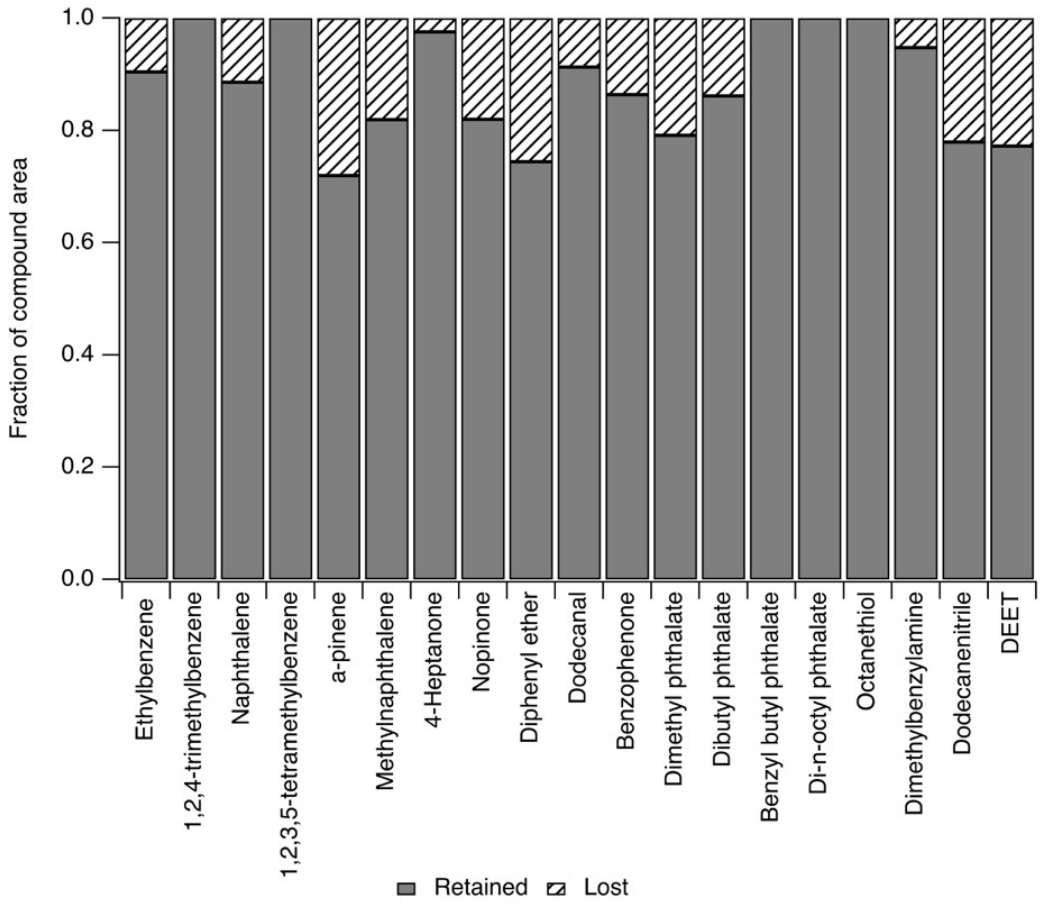

336 **Figure S4.** Evaluation of losses associated with adsorbent tube dry purge prior to tube desorption
337 and analysis. Peak areas from experiments using standards with and without a dry purge were
338 compared (y-axis). While some loss of volatile analytes is expected (Ochiai et al., 2014), most
339 analytes across a range of functional groups were retained reasonably well (~86% retained, on
340 average).

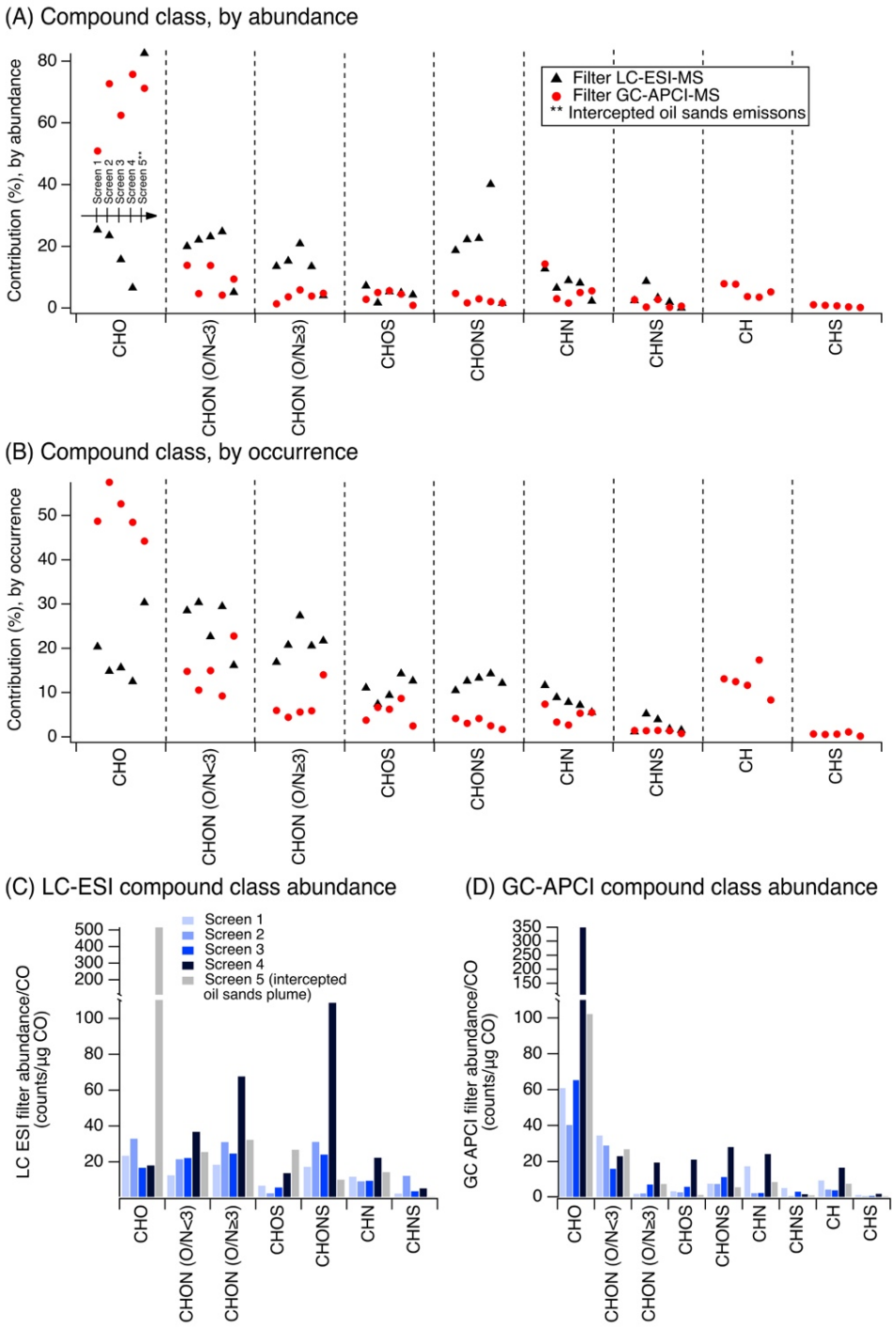

Figure S5. (A) Compound class distribution for particle-phase non-targeted LC-ESI-MS and GC-APCI-MS analyses, weighted by ion abundance. Percent contribution on the y-axis refers to each compound class' contribution to all observed compound ion abundance in LC or GC analysis. (B) For comparison, compound class distribution for particle-phase non-targeted LC-ESI-MS and GC-APCI-MS analyses, shown by occurrence (i.e. the number of compounds in each category—see Section S4 for further discussion). (C) Compound class distribution from particle-phase LC-ESI-MS analysis, and (D) compound class distribution from particle-phase

GC-APCI-MS analysis, both shown as raw ion abundance normalized by the average carbon monoxide measurement corresponding to the filter sampling period. In all panels, CH and CHS compounds are excluded from LC-ESI-MS analysis due to poor ESI ionization efficiency (Section S5). CH in GC-APCI-MS analysis may be underestimated due to known fragmentation of alkanes in the APCI source. This fragmentation is accounted for in the mass calibrated, targeted analysis of adsorbent tube compounds. These data are shown to support Figure 1A-B. GC-APCI-MS data from filter extracts are shown here for comparison with LC-ESI-MS data, but are not used in subsequent analyses. Differences between GC and LC results are due to differences in ionization techniques used in both methods (see Section S5) as well as changes in mixture composition that shift its GC- and LC-amenability.

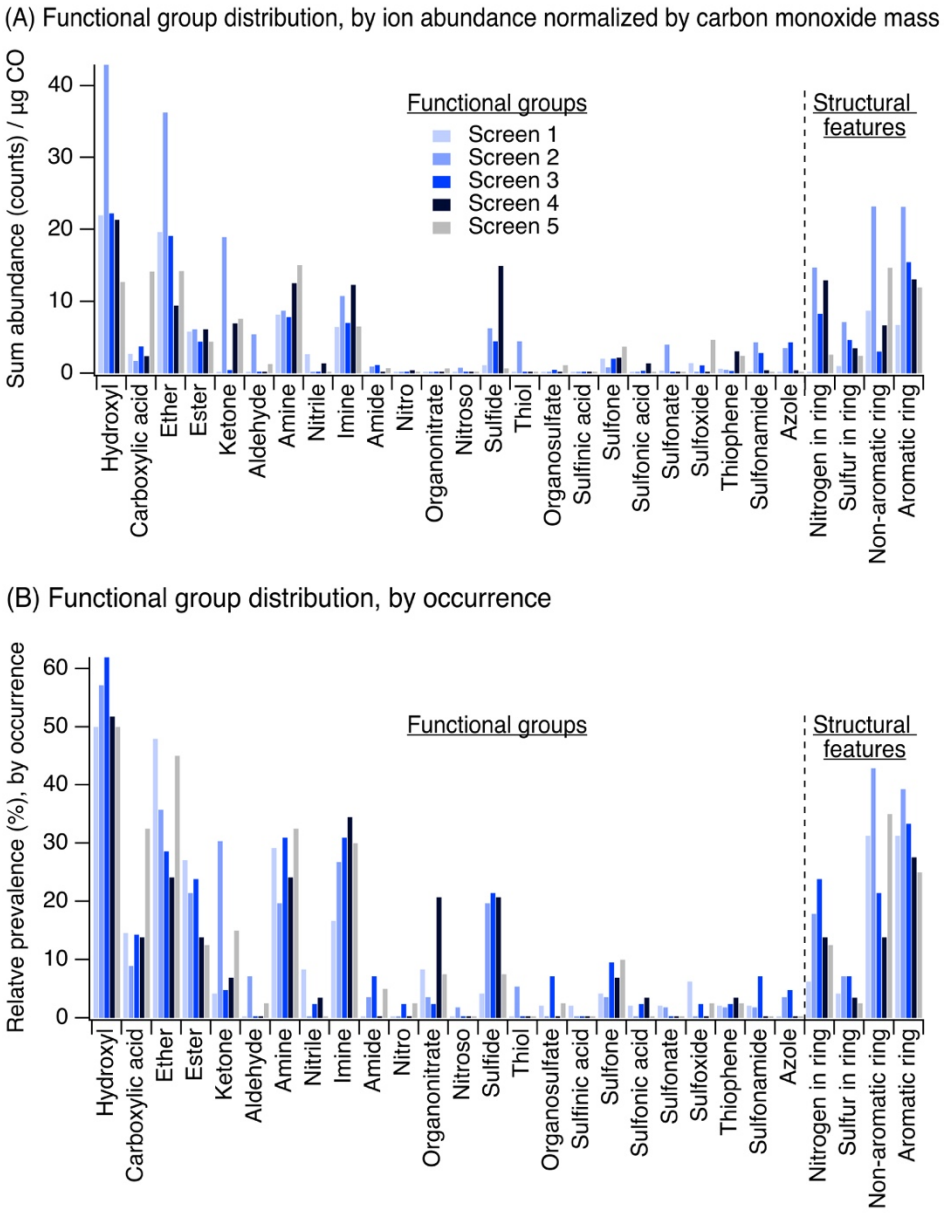

Figure S6. Functional group distribution of particle-phase functionalized OA from LC-ESI-MS/MS analysis represented (A) by raw abundance (normalized by carbon monoxide mass from corresponding sampling time) and (B) by occurrence (i.e. not weighted by abundance, not normalized by carbon monoxide—see Section S4 for further discussion). These data are shown to support Figure 1C.

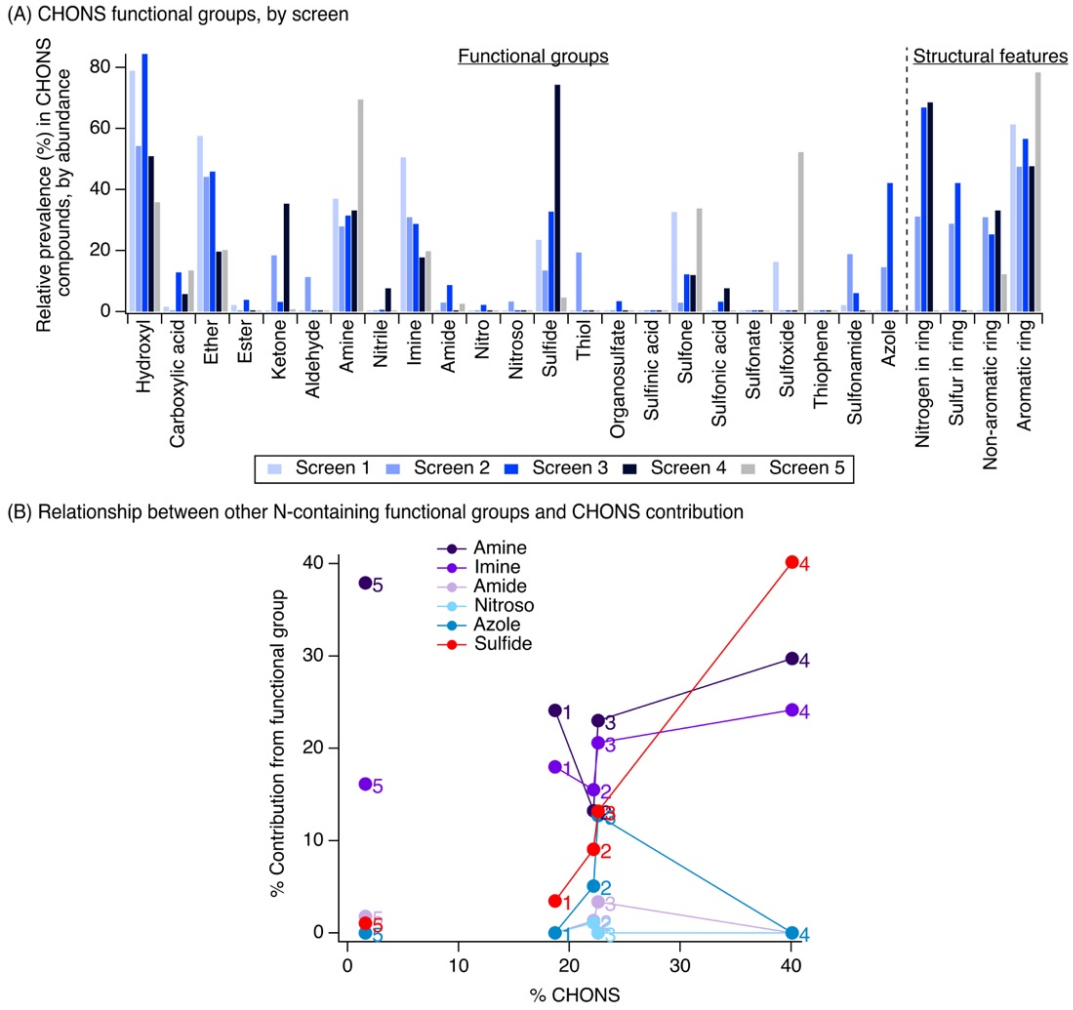

Figure S7. (A) Functional groups that contributed to CHONS compounds, weighted by abundance and shown by screen (shown to support Figure 2A-B). (B) Relationship between the contribution of amine, imine, amide, nitroso, azole, and sulfide groups to all functionalized OA and the contribution of the CHONS compound class prevalence. Numbers beside each marker represent screen number.

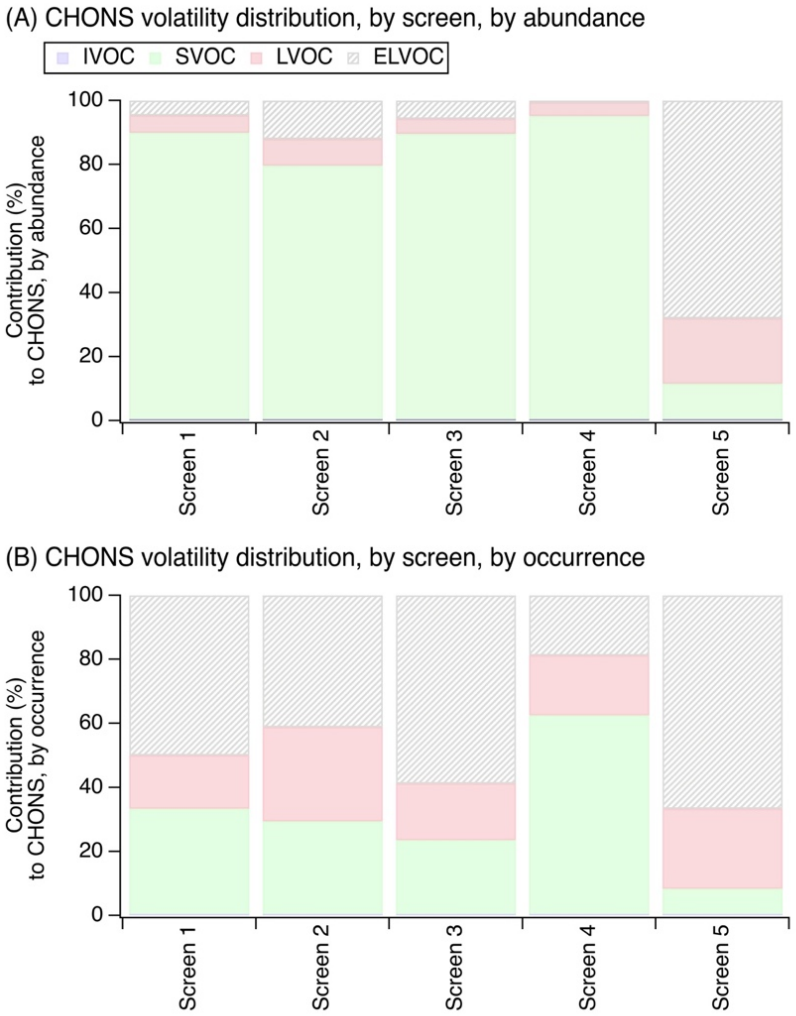

Figure S8. Volatility distribution of CHONS compounds, (A) shown by screen, weighted by abundance (to support Figure 2C), and (B) shown by occurrence (for comparison—see Section S4 for further discussion). Volatility was estimated using the parameterization in Li et al. (Li et al., 2016) and grouped into volatility bins following Li et al. and Donahue et al. (i.e. IVOC: 300 < C_0 < $3x10^6$ μg/m^3, SVOC: 0.3 < C_0 < 300 μg/m^3, LVOC: $3x10^{-4}$ < C_0 < 0.3 μg/m^3, ELVOC: C_0<10^{-4} (Donahue et al., 2011; Li et al., 2016)).

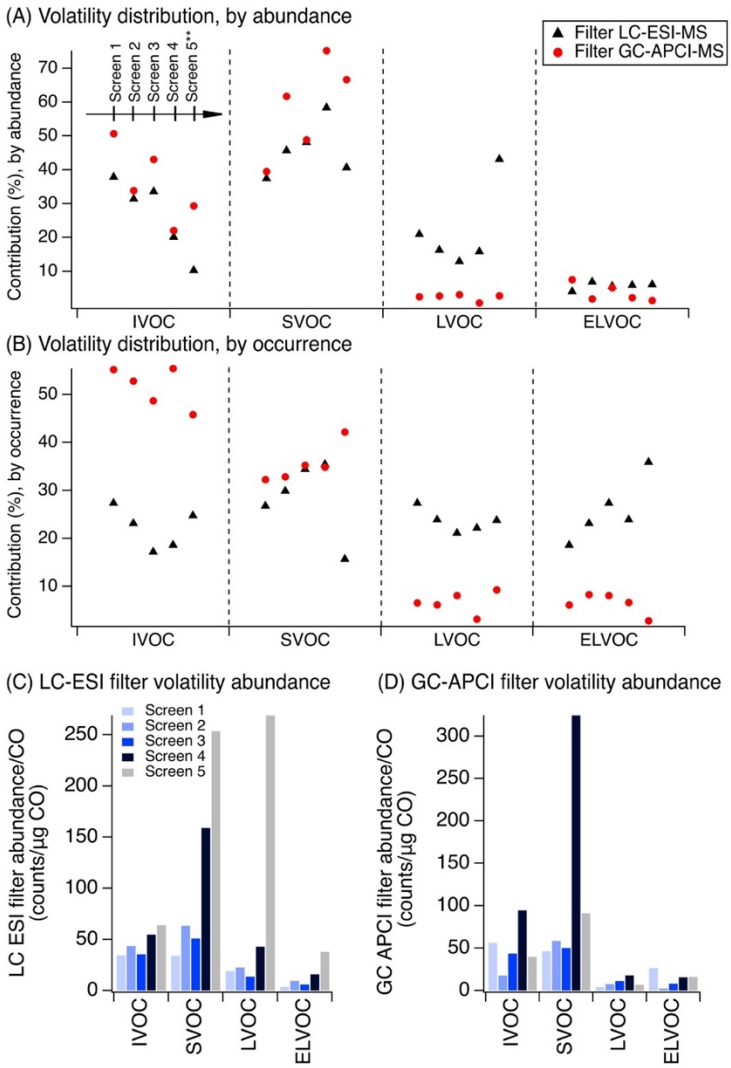

Figure S9. Volatility distribution of particle-phase compounds from non-targeted analysis, (A) weighted by abundance, (B) by occurrence (for comparison—see Section S4 for further discussion), (C) for particle-phase LC-ESI-MS samples, shown as raw abundance normalized by carbon monoxide, and (D) for particle-phase GC-APCI-MS samples, shown as raw abundance normalized by carbon monoxide. For (A-D), volatility was estimated using the parameterization in Li et al and grouped into volatility bins following Li et al. and Donahue et al. (i.e. IVOC: $300 < C_0 < 3x10^6$ µg/m^3, SVOC: $0.3 < C_0 < 300$ µg/m^3, LVOC: $3x10^{-4} < C_0 < 0.3$ µg/m^3, ELVOC: $C_0 < 10^{-4}$ (Donahue et al., 2011; Li et al., 2016)) .

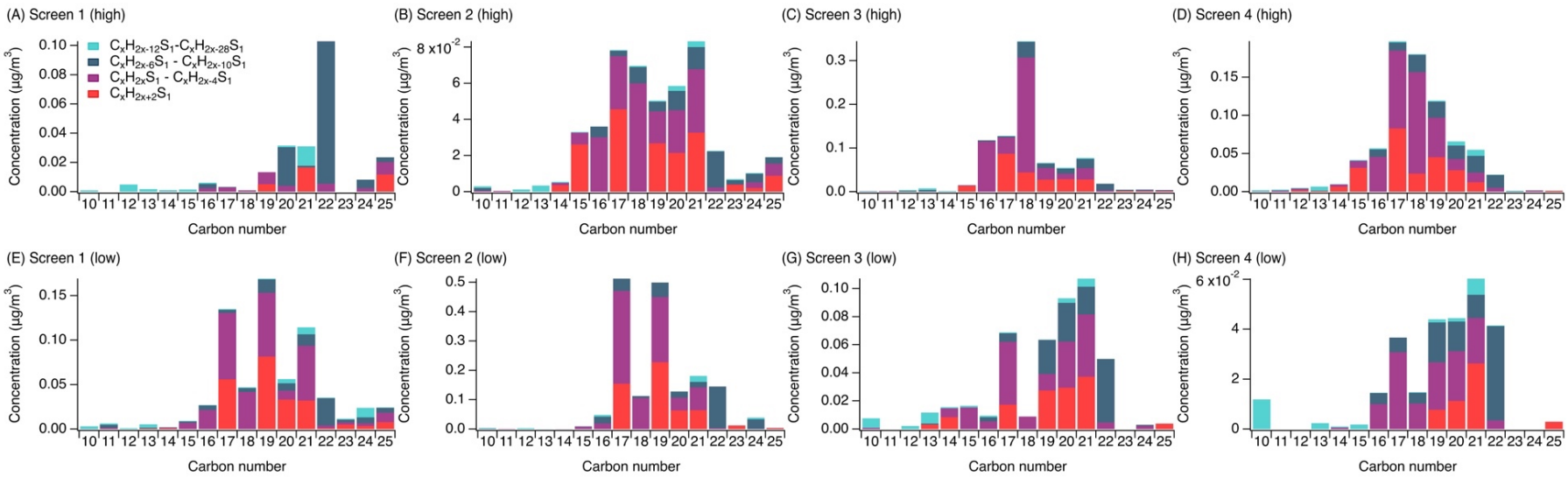

Figure S10. Distribution of carbon backbone structures for $C_xH_yS_1$ compounds collected on adsorbent tubes across screens 1-4, from targeted GC-APCI-MS analysis. Here, $C_xH_{2x+2}S_1$ represents saturated sulfur-containing compounds, $C_xH_{2x}S_1$- $C_xH_{2x-4}S_1$ represents sulfur-containing compounds with the equivalent of 1-3 double bonds and/or rings, $C_xH_{2x-6}S_1$- $C_xH_{2x-10}S_1$ represents sulfur-containing compounds with the equivalent of 4-6 double bonds and/or rings (e.g. single-ring aromatics), and $C_xH_{2x-12}S_1$-$C_xH_{2x-28}S_1$ represents sulfur-containing compounds with the equivalent of 7-15 double bonds and/or rings (e.g. PAHs). Screen 1 (low altitude) and screens 2, 3, and 4 (high altitude) showed the highest acetonitrile concentration, suggesting that the corresponding adsorbent tube samples were collected from the most concentrated portions of the plume (when comparing each low/high altitude pair at each screen). Values on each y-axis were not normalized by carbon monoxide measurements, to show absolute concentration measured on each adsorbent tube. To account for dilution, concentrations were normalized by carbon monoxide (e.g. Figure 4B). Mixing ratios are shown in Table S1.

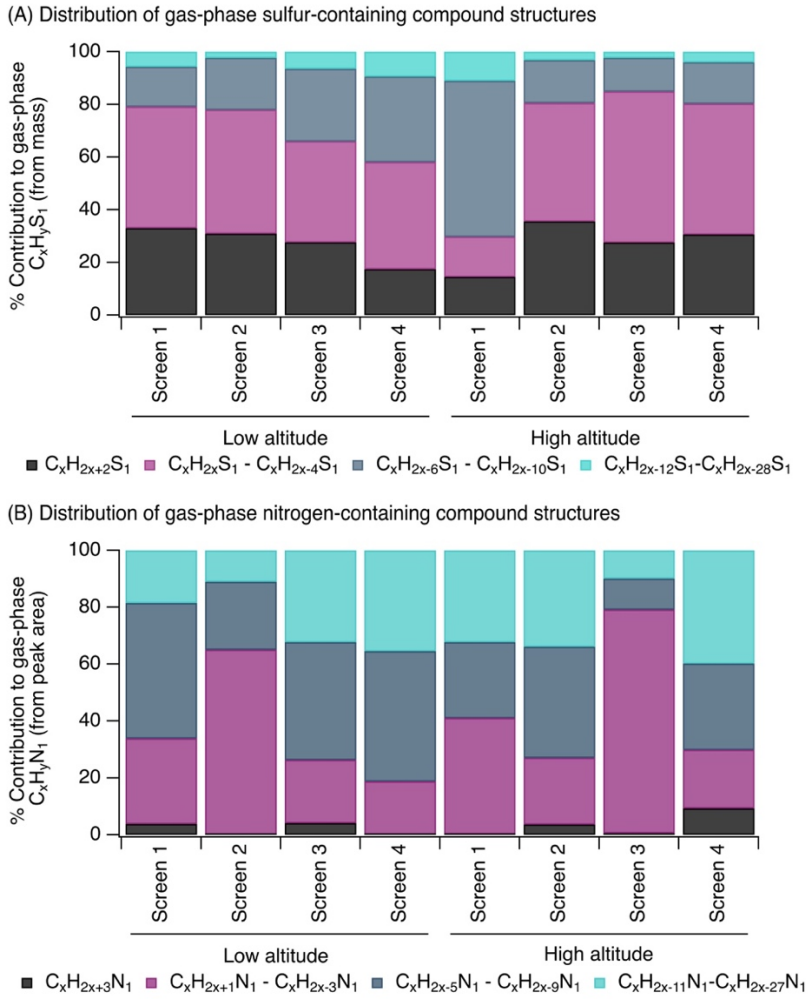

Figure S11. (A) Distribution of multiple bonds or ring structures for gas-phase $C_xH_yS_1$ compounds from targeted GC-APCI-MS analysis, where sulfur-containing compound peak areas were converted to mass as discussed in Section S3. (B) Distribution of multiple bonds or ring structures for gas-phase $C_xH_yN_1$ compounds from targeted GC-APCI-MS analysis. The nitrogen distribution was based on peak area. This contained a range of nitriles, pyrroles, pyridines, and other structures similar to past work (Akagi et al., 2011; Andreae, 2019; Gilman et al., 2015; Hatch et al., 2015; Koss et al., 2018). For (A-B), sulfur and nitrogen can form single or multiple bonds, so the presence of multiple bonds or rings may be in the carbon backbone structure or on the sulfur/nitrogen heteroatom. Here, black bars represent saturated compounds, pink bars represent those with the equivalent of 1-3 double bonds and/or rings, dark teal bars represent those with the equivalent of 4-6 double bonds and/or rings (e.g. single ring aromatics), and light teal bars represent those with the equivalent of 7-15 double bonds and/or rings (e.g. PAHs).

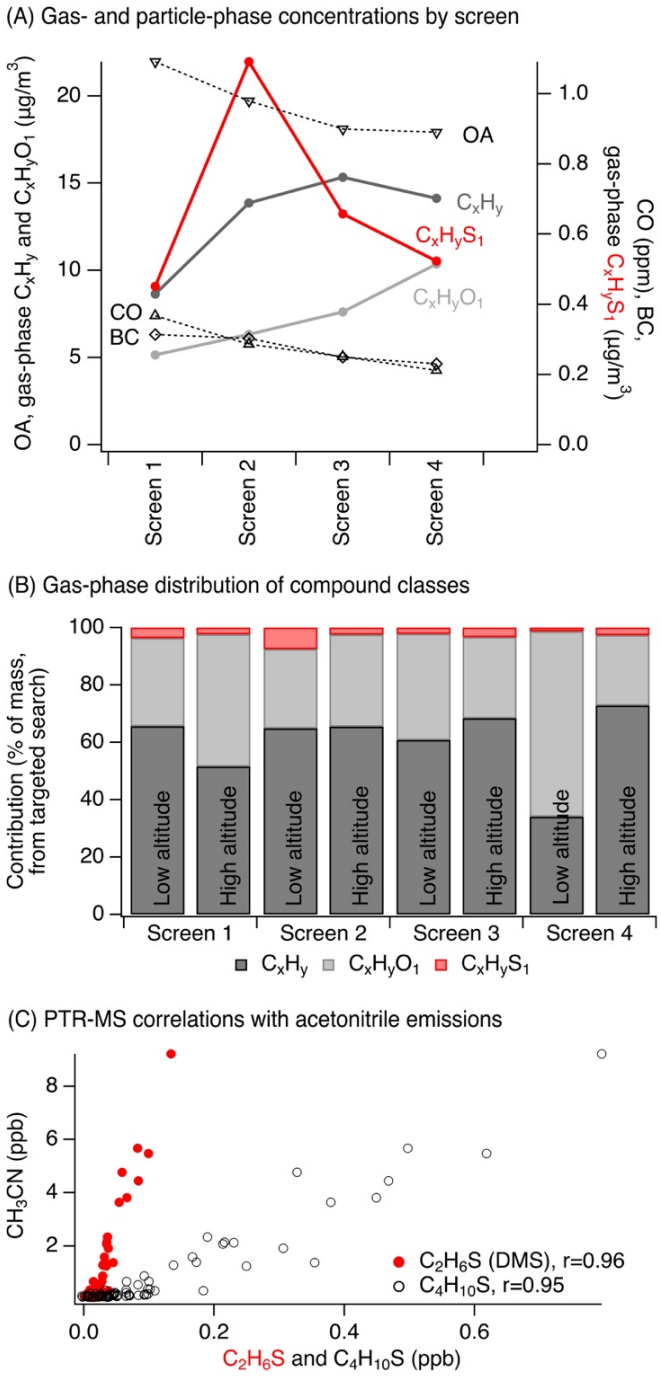

404 **Figure S12.** (A) Concentration of gas-phase C_xH_y, $C_xH_yO_1$, and $C_xH_yS_1$ compounds, BC, OA
405 from AMS, and CO as tracers of plume dilution (shown to support Figure 4B, concentrations not
406 normalized by carbon monoxide here). (B) Relative contribution of C_xH_y, $C_xH_yO_1$, and $C_xH_yS_1$
407 compounds from the targeted search in the gas phase (C_{10}-C_{25}) from GC-APCI-MS analysis.
408 C_xH_y, $C_xH_yO_1$, and $C_xH_yS_1$ contributions were converted to mass concentrations prior to
409 analysis. $C_xH_yN_1$ was not included here because $C_xH_yN_1$ was examined in terms of peak area
410 only. (C) Correlation between concentration of C_2H_6S (dimethylsulfide (DMS) and isomers) and
411 $C_4H_{10}S$ (diethylsulfide and isomers) versus acetonitrile from aircraft PTR-ToF-MS data.

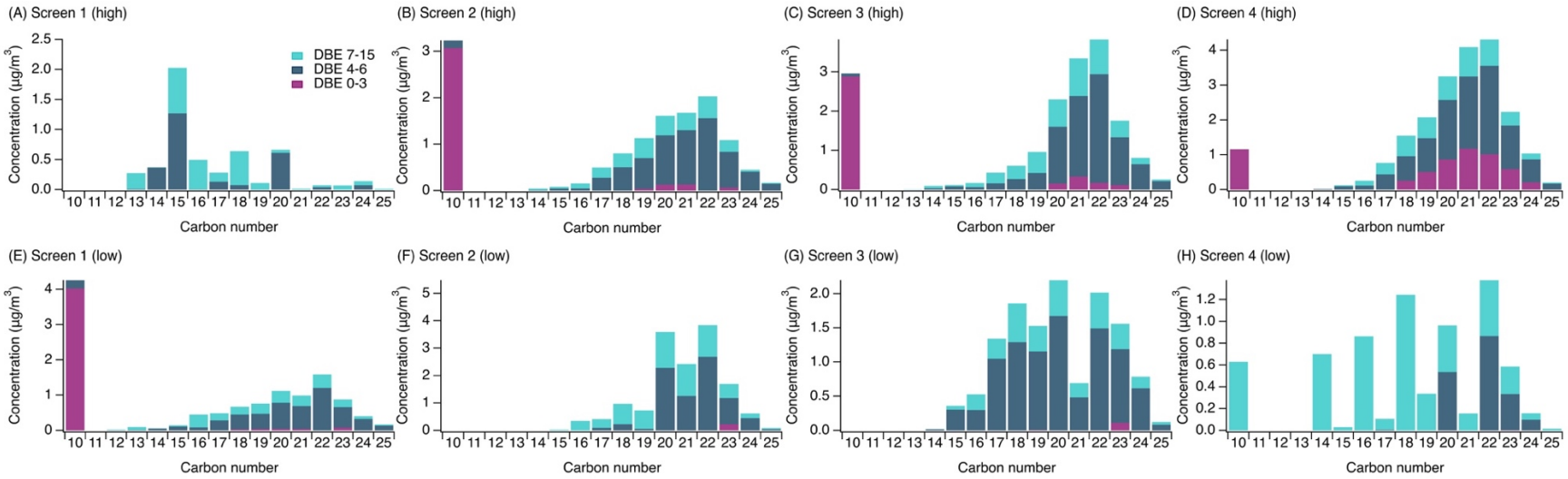

Figure S13. Distribution of carbon backbone structures for gas-phase C_xH_y hydrocarbons collected on adsorbent tubes across screens 1-4 (from targeted GC-APCI-MS analysis). DBE 0-3 represents alkanes, alkenes, and cyclic alkanes. DBE 4-6 represents single ring aromatics. DBE 7-15 represents polycyclic aromatics hydrocarbons (PAHs). The observed C_{10} compounds classified as DBE 0-3 (pink) were dominated by monoterpenes. Screen 1 (low altitude) and screens 2, 3, and 4 (high altitude) showed the highest acetonitrile concentration, suggesting that the corresponding adsorbent tube samples were collected from the most concentrated portions of the plume. Values on each y-axis were not normalized by carbon monoxide measurements, to show absolute concentration measured on each adsorbent tube. To account for dilution, concentrations were normalized by carbon monoxide (e.g. Figure 4B). Mixing ratios are shown in Table S1.

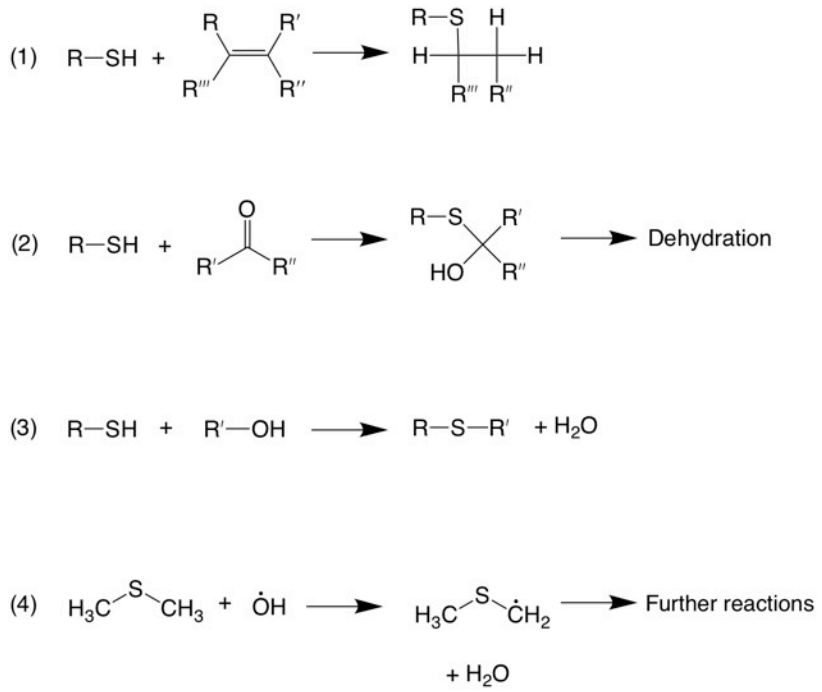

Figure S14. Possible reaction pathways from the literature, including (1) a thiol-ene reaction (Lowe, 2010), (2) reaction with a carbonyl (Jencks and Lienhard, 1966), (3) reaction with an alcohol (Mashkina, 1991), and (4) hydrogen abstraction from dimethyl sulfide (Barnes et al., 2006).

Table S1. Summary table of average flow rates, sampling times, and CO mixing ratios (ppm displayed here for ease of interpretation, but values in $\mu g/m^3$ were used to normalize ion abundances (counts/m^3) or mass concentrations ($\mu g/m^3$)).

Adsorbent tubes				
Sample	Average flow rate (sccm)	Sampling time (min)	Average altitude (m)	Average CO during sampling (ppm)
Screen 1, low altitude	288	52.3	655	0.486
Screen 2, low altitude	276	6.60	641	0.148
Screen 3, low altitude	285	9.15	809	0.109
Screen 4, low altitude	291	4.10	727	0.184
Screen 1, high altitude	278	4.70	915	0.141
Screen 2, high altitude	280	44.0	1172	0.457
Screen 3, high altitude	282	47.0	962	0.389
Screen 4, high altitude	296	30.1	1645	0.277
Filters				
Sample	Average flow rate (slpm)	Sampling time (min)	Average altitude (m)	Average CO during sampling (ppm)
Screen 1	47	52.4	1115	0.492
Screen 2	46	44.0	1287	0.469
Screen 3	46	47.0	1268	0.409
Screen 4	47	29.1	932	0.296
Screen 5	44	101.0	1608	0.186

Table S2. Fraction of hydrocarbons from adsorbent tubes in the gas- vs. particle-phase, based on AMS OA concentration (18-22 μg/m^3, averaged across low and high altitude adsorbent tube sampling times) and the effective saturation concentration of hydrocarbons in the carbon number range of interest (Donahue et al., 2009, 2011).

C^* (μg/m^3)	$Log_{10}(C^*)$ (μg/m^3)	Number of carbon atoms	Fraction in the gas phase	Fraction in particle phase
1000000	6.00	12.4	1.00	0.00
100000	5.00	14.5	1.00	0.00
10000	4.00	16.6	1.00	0.00
1000	3.00	18.7	0.98	0.02
100	2.00	20.8	0.84	0.16
50	1.70	21.4	0.72	0.28
30	1.48	21.9	0.61	0.39
20	1.30	22.3	0.51	0.49
10	1.00	22.9	0.34	0.66
1	0.00	25.0	0.05	0.95

Table S3. Comparison of AMS OA concentration and total targeted gas-phase C_xH_y, $C_xH_yO_1$, $C_xH_yS_1$ compound concentration, shown as a change between screens 1 and 2. Columns show concentration difference and the ratio of targeted gas-phase compound concentration difference to carbon monoxide concentration difference.

Screen 1→2	Concentration difference	Ratio of concentration difference to CO concentration difference
AMS OA	-2.3 μg/m^3	-0.0044 (7% decrease)
Σ(C_xH_y, $C_xH_yO_1$, $C_xH_yS_1$) from targeted adsorbent tube search	+7.0 μg/m^3	+0.022 (55% increase)

References

Akagi, S. K., Yokelson, R. J., Wiedinmyer, C., Alvarado, M. J., Reid, J. S., Karl, T., Crounse, J. D. and Wennberg, P. O.: Emission factors for open and domestic biomass burning for use in atmospheric models, Atmos. Chem. Phys., 11(9), 4039–4072, doi:10.5194/acp-11-4039-2011, 2011.

Andreae, M. O.: Emission of trace gases and aerosols from biomass burning – An updated assessment, Atmos. Chem. Phys., 1–27, doi:10.5194/acp-2019-303, 2019.

Barnes, I., Hjorth, J. and Mihalapoulos, N.: Dimethyl sulfide and dimethyl sulfoxide and their oxidation in the atmosphere, Chem. Rev., 106(3), 940–975, doi:10.1021/cr020529+, 2006.

Corrigan, A. L., Russell, L. M., Takahama, S., Äijälä, M., Ehn, M., Junninen, H., Rinne, J., Petäjä, T., Kulmala, M., Vogel, A. L., Hoffmann, T., Ebben, C. J., Geiger, F. M., Chhabra, P., Seinfeld, J. H., Worsnop, D. R., Song, W., Auld, J. and Williams, J.: Biogenic and biomass burning organic aerosol in a boreal forest at Hyytiälä, Finland, during HUMPPA-COPEC 2010, Atmos. Chem. Phys., 13(24), 12233–12256, doi:10.5194/acp-13-12233-2013, 2013.

Ditto, J. C., Barnes, E. B., Khare, P., Takeuchi, M., Joo, T., Bui, A. A. T., Lee-Taylor, J., Eris, G., Chen, Y., Aumont, B., Jimenez, J. L., Ng, N. L., Griffin, R. J. and Gentner, D. R.: An omnipresent diversity and variability in the chemical composition of atmospheric functionalized organic aerosol, Commun. Chem., 1(1), 75, doi:10.1038/s42004-018-0074-3, 2018.

Ditto, J. C., Joo, T., Khare, P., Sheu, R., Takeuchi, M., Chen, Y., Xu, W., Bui, A. A. T., Sun, Y., Ng, N. L. and Gentner, D. R.: Effects of Molecular-Level Compositional Variability in

458 Organic Aerosol on Phase State and Thermodynamic Mixing Behavior, Environ. Sci.
459 Technol., 53(22), 13009–13018, doi:10.1021/acs.est.9b02664, 2019.
460 Ditto, J. C., Joo, T., Slade, J. H., Shepson, P. B., Ng, N. L. and Gentner, D. R.: Nontargeted
461 Tandem Mass Spectrometry Analysis Reveals Diversity and Variability in Aerosol
462 Functional Groups across Multiple Sites, Seasons, and Times of Day, Environ. Sci.
463 Technol. Lett., 7(2), 60–69, doi:10.1021/acs.estlett.9b00702, 2020.
464 Donahue, N. M., Robinson, A. L. and Pandis, S. N.: Atmospheric organic particulate matter:
465 From smoke to secondary organic aerosol, Atmos. Environ., 43(1), 94–106,
466 doi:10.1016/j.atmosenv.2008.09.055, 2009.
467 Donahue, N. M., Epstein, S. A., Pandis, S. N. and Robinson, A. L.: A two-dimensional volatility
468 basis set: 1. organic-aerosol mixing thermodynamics, Atmos. Chem. Phys., 11(7), 3303–
469 3318, doi:10.5194/acp-11-3303-2011, 2011.
470 Gilman, J. B., Lerner, B. M., Kuster, W. C., Goldan, P. D., Warneke, C., Veres, P. R., Roberts, J.
471 M., De Gouw, J. A., Burling, I. R. and Yokelson, R. J.: Biomass burning emissions and
472 potential air quality impacts of volatile organic compounds and other trace gases from
473 fuels common in the US, Atmos. Chem. Phys., 15(24), 13915–13938, doi:10.5194/acp-
474 15-13915-2015, 2015.
475 Hatch, L. E., Luo, W., Pankow, J. F., Yokelson, R. J., Stockwell, C. E. and Barsanti, K. C.:
476 Identification and quantification of gaseous organic compounds emitted from biomass
477 burning using two-dimensional gas chromatography-time-of-flight mass spectrometry,
478 Atmos. Chem. Phys., 15(4), 1865–1899, doi:10.5194/acp-15-1865-2015, 2015.
479 Jencks, W. P. and Lienhard, G. E.: Thiol Addition to the Carbonyl Group. Equilibria and
480 Kinetics, J. Am. Chem. Soc., 88(17), 3982–3995, doi:10.1021/ja00969a017, 1966.

Khare, P., Marcotte, A., Sheu, R., Walsh, A. N., Ditto, J. C. and Gentner, D. R.: Advances in offline approaches for trace measurements of complex organic compound mixtures via soft ionization and high-resolution tandem mass spectrometry, J. Chromatogr. A, 1598, 163–174, doi:10.1016/j.chroma.2019.03.037, 2019.

Khare, P., Machesky, J., Soto, R., He, M., Presto, A. A. and Gentner, D. R.: Asphalt-related emissions are a major missing nontraditional source of secondary organic aerosol precursors, Sci. Adv., 6(36), doi:10.1126/sciadv.abb9785, 2020.

Kondyli, A. and Schrader, W.: Evaluation of the combination of different atmospheric pressure ionization sources for the analysis of extremely complex mixtures, Rapid Commun. Mass Spectrom., 34(8), 1–9, doi:10.1002/rcm.8676, 2019.

Koss, A. R., Sekimoto, K., Gilman, J. B., Selimovic, V., Coggon, M. M., Zarzana, K. J., Yuan, B., Lerner, B. M., Brown, S. S., Jimenez, J. L., Krechmer, J., Roberts, J. M., Warneke, C., Yokelson, R. J. and De Gouw, J.: Non-methane organic gas emissions from biomass burning: Identification, quantification, and emission factors from PTR-ToF during the FIREX 2016 laboratory experiment, Atmos. Chem. Phys., 18(5), 3299–3319, doi:10.5194/acp-18-3299-2018, 2018.

Kroll, J. H., Donahue, N. M., Jimenez, J. L., Kessler, S. H., Canagaratna, M. R., Wilson, K. R., Altieri, K. E., Mazzoleni, L. R., Wozniak, A. S., Bluhm, H., Mysak, E. R., Smith, J. D., Kolb, C. E. and Worsnop, D. R.: Carbon oxidation state as a metric for describing the chemistry of atmospheric organic aerosol., Nat. Chem., 3(2), 133–139, doi:10.1038/nchem.948, 2011.

Li, S. M., Leithead, A., Moussa, S. G., Liggio, J., Moran, M. D., Wang, D., Hayden, K., Darlington, A., Gordon, M., Staebler, R., Makar, P. A., Stroud, C. A., McLaren, R., Liu,

P. S. K., O'Brien, J., Mittermeier, R. L., Zhang, J., Marson, G., Cober, S. G., Wolde, M. and Wentzell, J. J. B.: Differences between measured and reported volatile organic compound emissions from oil sands facilities in Alberta, Canada, Proc. Natl. Acad. Sci. U. S. A., 114(19), E3756–E3765, doi:10.1073/pnas.1617862114, 2017.

Li, Y., Pöschl, U. and Shiraiwa, M.: Molecular corridors and parameterizations of volatility in the chemical evolution of organic aerosols, Atmos. Chem. Phys., 16(5), 3327–3344, doi:10.5194/acp-16-3327-2016, 2016.

Lowe, A. B.: Thiol-ene "click" reactions and recent applications in polymer and materials synthesis, Polym. Chem., 1(1), 17–36, doi:10.1039/b9py00216b, 2010.

Mashkina, A. V.: Catalytic Synthesis Of Sulfides Sulfoxides and Sulfones, Sulfur reports, 10(4), 279–388, doi:10.1080/01961779108048759, 1991.

Middlebrook, A. M., Bahreini, R., Jimenez, J. L. and Canagaratna, M. R.: Evaluation of composition-dependent collection efficiencies for the Aerodyne aerosol mass spectrometer using field data, Aerosol Sci. Technol., 46(3), 258–271, doi:10.1080/02786826.2011.620041, 2012.

Ng, N. L., Kwan, A. J., Surratt, J. D., Chan, A. W. H., Chhabra, P. S., Sorooshian, A., Pye, H. O. T., Crounse, J. D., Wennberg, P. O., Flagan, R. C. and Seinfeld, J. H.: Secondary organic aerosol (SOA) formation from reaction of isoprene with nitrate radicals (NO3), Atmos. Chem. Phys., 8, 4117–4140, 2008.

Ochiai, N., Tsunokawa, J., Sasamoto, K. and Hoffmann, A.: Multi-volatile method for aroma analysis using sequential dynamic headspace sampling with an application to brewed coffee, J. Chromatogr. A, 1371, 65–73, doi:10.1016/j.chroma.2014.10.074, 2014.

Riva, M., Da Silva Barbosa, T., Lin, Y.-H., Stone, E. A., Gold, A., Surratt, J. D., Barbosa, T. D.

S., Lin, Y.-H., Stone, E. A. and Gold, A.: Characterization of organosulfates in secondary organic aerosol derived from the photooxidation of long-chain alkanes, Atmos. Chem. Phys., 16, 11001–11018, doi:10.5194/acp-2016-20, 2016a.

Riva, M., Budisulistiorini, S. H., Chen, Y., Zhang, Z., D'Ambro, E. L., Zhang, X., Gold, A., Turpin, B. J., Thornton, J. A., Canagaratna, M. R. and Surratt, J. D.: Chemical Characterization of Secondary Organic Aerosol from Oxidation of Isoprene Hydroxyhydroperoxides, Environ. Sci. Technol., 50, 9889–9899, doi:10.1021/acs.est.6b02511, 2016b.

Schauer, J. J., Kleeman, M. J., Cass, G. R. and Simoneit, B. R. T.: Measurement of emissions from air pollution sources. 3. C1-C29 organic compounds from fireplace combustion of wood, Environ. Sci. Technol., 35(9), 1716–1728, doi:10.1021/es001331e, 2001.

Seinfeld, J. H., Surratt, J. D., Gomez-Gonzalez, Y., Chan, A. W. H., Vermeylen, R., Shahgholi, M., Kleindienst, T. E., Edney, E. O., Offenberg, J. H., Lewandowski, M., Jaoui, M., Maenhaut, W., Claeys, M., Flagan, R. C. and Seinfeld, J. H.: Organosulfate Formation in Biogenic Secondary Organic Aerosol, J. Phys. Chem. A, 112(36), 8345–8378, doi:Doi 10.1021/Jp802310p, 2008.

Sheu, R., Marcotte, A., Khare, P., Charan, S., Ditto, J. C. and Gentner, D. R.: Advances in offline approaches for chemically speciated measurements of trace gas-phase organic compounds via adsorbent tubes in an integrated sampling-to-analysis system, J. Chromatogr. A, 1575, 80–90, doi:10.1016/j.chroma.2018.09.014, 2018.

Simoneit, B. R. T., Rogge, W. F., Mazurek, M. A., Standley, L. J., Hildemann, L. M. and Cass, G. R.: Lignin Pyrolysis Products, Lignans, and Resin Acids as Specific Tracers of Plant Classes in Emissions from Biomass Combustion, Environ. Sci. Technol., 27(12), 2533–

2541, doi:10.1021/es00048a034, 1993.

Worton, D. R., Zhang, H., Isaacman-Vanwertz, G., Chan, A. W. H. H., Wilson, K. R. and Goldstein, A. H.: Comprehensive Chemical Characterization of Hydrocarbons in NIST Standard Reference Material 2779 Gulf of Mexico Crude Oil, Environ. Sci. Technol., 49(22), 13130–13138, doi:10.1021/acs.est.5b03472, 2015.

Zhou, S., Collier, S., Jaffe, D. A., Briggs, N. L., Hee, J., Iii, A. J. S., Kleinman, L., Onasch, T. B. and Zhang, Q.: Regional influence of wildfires on aerosol chemistry in the western US and insights into atmospheric aging of biomass burning organic aerosol, Atmos. Chem. Phys., 17(3), 2477–2493, doi:10.5194/acp-17-2477-2017, 2017.